

Cite this: *J. Mater. Chem. A*, 2020, **8**, 7066

# Heavy oil-derived carbon for energy storage applications

Han Hu  and Mingbo Wu \*

In the past decade, renewable energy has been a hot pursuit in scientific and industrial communities because of the fast depletion of fossil fuels and increasing concern about the environment. To efficiently utilize and largely deploy the intermittent renewable energy, high-performance electrochemical energy storage devices are desperately needed. As a result, tremendous effort has been devoted to this field with remarkable achievements. Despite this progress, fossil fuels, like petroleum, will still play an indispensable role in our energy structure in the foreseeable future. Besides, petroleum is becoming increasingly heavier and the heavy oil results in more and more low-value by-products such as asphalt and petroleum coke during the oil refinery processes. In this context, how to harmonize the deployment of renewable energy and value-added utilization of these abundant and low-cost by-products from the petroleum industry represents a significant challenge. Considering their high carbon content and versatile tunability, one viable solution may be the controllable conversion of asphalt and/or petroleum coke into functional carbon materials for energy storage applications. In this article, we summarize the recent progress of carbon materials derived from heavy oil by-products and their utilization as electrode materials for energy storage devices. At first, we give a brief introduction to the features and advantages of heavy oil by-products compared to biomass and polymers as the precursors of carbon materials. Then, the typical methods of constructing functional carbon materials from these by-products are discussed in detail. After that, their performance as electrode materials for lithium-ion batteries, sodium-ion batteries, and supercapacitors is elaborately presented. Finally, the possible challenges and future perspectives are analyzed based on our knowledge to end this review.

Received 3rd January 2020  
Accepted 13th March 2020

DOI: 10.1039/d0ta00095g

[rsc.li/materials-a](https://rsc.li/materials-a)

State Key Laboratory of Heavy Oil Processing, College of Chemical Engineering, College of New Energy, Institute of New Energy, China University of Petroleum (East China), Qingdao 266580, China. E-mail: [wumb@upc.edu.cn](mailto:wumb@upc.edu.cn)



*Dr Mingbo Wu is a professor and executive president of College of New Energy, China University of Petroleum (East China). His research interests have been focused on the development of new methodologies for the synthesis of functional carbon materials, and their uses in catalysis, energy conversion/storage and environmental protection. He has received a number of awards, including*

*the First Class Award for achievements in technological invention from the China Petroleum and Chemical Industry Foundation, the Runners-up Award for achievements in technological invention from the Education Ministry of China, and so on. He has published more than 160 papers in peer-reviewed journals.*

## 1. Introduction

In the past 100 years, the development of our world has been largely dependent on the overconsumption of non-renewable fossil fuels.<sup>1,2</sup> This unsustainable development has resulted in serious resource shortage, environmental pollution, and global warming.<sup>3–8</sup> To address these severe issues, our society is actively moving towards alternative resources with renewability and sustainability.<sup>9–13</sup> In this regard, an increasing amount of world energy has been produced from the sun and wind in the past few years.<sup>14,15</sup> However, renewable energy is generally produced intermittently, and its efficient utilization strongly relies on energy storage systems.<sup>8,16,17</sup> Thus far, tremendous research efforts have been devoted to exploring high-performance energy storage systems with remarkable progress achieved, as evident by the popularity of lithium-ion batteries, sodium-ion batteries, supercapacitors, *etc.*<sup>18–26</sup> As the key component of energy storage systems, energy storage materials play a pivotal role in determining their performance, thus making the development of energy storage materials one of the most active research fields recently.<sup>27–30</sup> Among all the available candidates, carbon materials have received focused attention because of their wide availability, diverse tunability,

high conductivity, and excellent stability.<sup>31</sup> Tremendous efforts devoted to this field have led to a wealth of novel nanostructured carbon materials with excellent performance for energy storage applications.<sup>32–34</sup> However, most of the promising results remain at the stage of laboratory studies. One main reason is that these novel carbon materials are mainly produced using expensive polymers as the precursors, which inevitably increases the cost of final products.<sup>35</sup> The employment of widely available and renewable biomass to produce carbon materials for energy storage offers an alternative strategy to alleviate the limitation of polymer precursors.<sup>36</sup> By rationally selecting biomass precursors, carbon materials with multiple structures and morphologies have been produced and successfully utilized as electrode materials for a wealth of energy storage devices.<sup>32,36</sup> Nevertheless, biomass generally shows well-defined structures, offering very limited possibilities to manipulate the structures of final carbon materials during the manufacturing process. Suitable biomass precursors for carbon materials with desired properties have to be determined using low-efficient trial and error processes. Besides, biomass is largely influenced by season and region which may impose a significant challenge for precursor management. As a result, biomass still cannot fully fulfil the diverse requirements of energy storage systems on carbon materials and precursors with low-cost and high tunability still need to be actively exploited.<sup>37</sup>

The percentage of fossil fuels, for example petroleum, in our energy structure is gradually decreasing because of the rapid development of renewable and sustainable energy.<sup>38</sup> Nevertheless, petroleum will still play an indispensable role in modern society in the foreseeable future.<sup>39–41</sup> The petroleum industry is the largest industry which not only produces fuels to power vehicles but also contributes to a multitude of products penetrating deeply into almost all aspects of our life.<sup>39,40</sup> Due to excessive consumption of petroleum resources for a long duration, a very serious situation we have to face now is that the crude oil supplied for the petroleum industry is becoming heavier and heavier, which inevitably results in the production of an increasing number of low-value and extremely heavy by-products, such as asphalt and petroleum coke.<sup>39,40</sup> As a result, the effective utilization of these heavy by-products presents a formidable challenge for today's petroleum industry.<sup>42</sup> The heavy by-products generally contain a very high content of carbon which mainly exists in the form of polycyclic aromatic hydrocarbons (PAHs), a class of organic compounds made of two or more fused aromatic rings.<sup>42–45</sup> These compounds have been regarded as the fundamental subunits of graphene and its derivatives that can possibly result in the formation of a broad spectrum of functional carbon nanomaterials.<sup>46</sup> Compared to their counterparts from biomass and/or polymer precursors, PAH derived carbons hold higher conductivity and tunability.<sup>47</sup> Moreover, asphalt is normally carbonized through a liquid-phase process which provides multiple opportunities for elaborately manipulating the structure of the final carbon materials.<sup>22,37</sup> These features make the heavy by-products from the petroleum industry excellent precursors to construct novel nanostructured carbons.

Oil-derived heavy by-products have been used to prepare carbon materials for a while.<sup>48–52</sup> Typical examples include activated carbon and carbon fibres from petroleum coke and asphalt, respectively.<sup>53–55</sup> With the development of nanotechnology in recent years,<sup>56</sup> these precursors have been extended to construct novel nanostructured carbon materials with wide applications and their potential for energy storage has been successfully demonstrated.<sup>22,57</sup> Because of the aforementioned advantages of the oil-derived heavy by-products, the structural details of the as-prepared carbon nanomaterials can be elaborately modulated.<sup>37</sup> In this regard, the current heavy oil-derived by-products can serve as promising precursors for the cost-effective production of energy storage carbon materials. Our group has been actively engaged in this field for years. Through innovative yet simple approaches, zero-dimensional carbon quantum dots, one-dimensional carbon nanofibres, two-dimensional carbon nanosheets, and three-dimensional carbon frameworks have been successfully prepared.<sup>58–61</sup> The rich tunability of heavy oil-derived precursors, as well as their low-cost and wide availability, makes them more competitive in producing novel nanostructured carbon materials compared to biomass and polymer precursors. As a result, a timely summary of recent progress in this field is urgently required. In this review, we first give a brief introduction to the typical heavy oil-derived precursors, such as asphalt and petroleum coke, for novel nanostructured carbon materials. Then, innovative strategies for modulating their morphology, porosity, specific surface area, conductivity, and so on are discussed in detail. After that, the progress of these novel carbon nanomaterials as electrode materials for lithium-ion batteries, sodium-ion batteries, and supercapacitors is presented. Finally, we conclude this review with the urgent challenges and promising prospects of heavy oil-derived nanostructured carbon materials for energy storage applications.

## 2. Typical heavy by-products from crude oil

Petroleum cannot be directly used but serves as the feedstock that must be processed into light fuels to power vehicles and petrochemicals for many industries.<sup>39,40</sup> The main aims of the modern refinery are to harvest as many fuels and chemicals as possible from the crude oil. In addition to these valued products, quite some low-value and heavy by-products are also generated. As the worldwide crude oil is getting heavier, abundant heavy by-products are inevitably produced.<sup>39</sup>

Despite the diversity of the refinery processes, they can be simply categorized as separation and conversion ones.<sup>40</sup> The typical heavy residue from the separation processes, for example distillation, is asphalt, a complex mixture of saturates, aromatics, resins, and asphaltenes, as shown in Fig. 1.<sup>62,63</sup> Asphalt can be either hard or soft and even liquid, depending on the relative content of the aforementioned four fractions. The typical structure of the four fractions is illustrated in Fig. 1. Most of them are made of PAHs, which can condense into large graphene domains.<sup>57</sup> This provides the

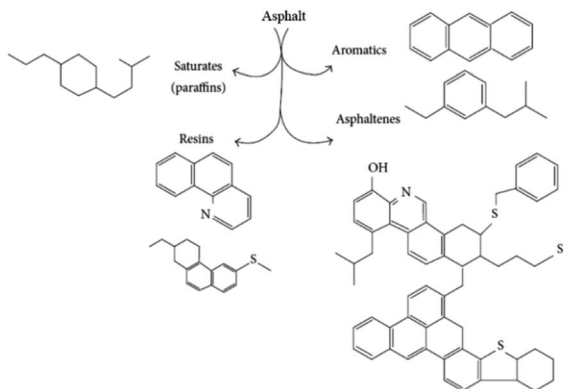


Fig. 1 Representative structures of asphalt fractions. (Permission from ref. 62, Copyright 2014, Hindawi.)

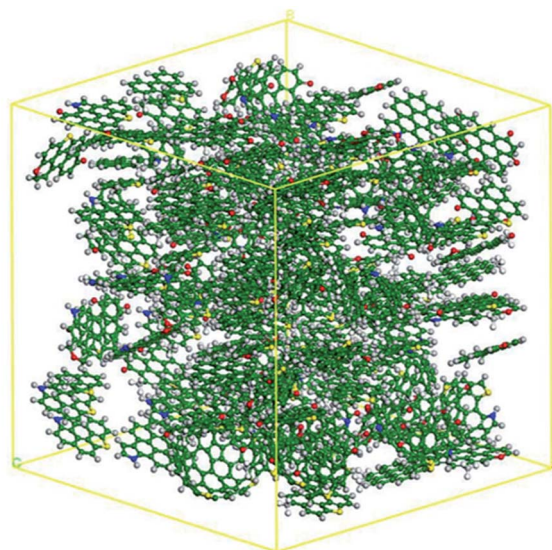


Fig. 2 Structural model of a typical petroleum coke. The carbon, oxygen, sulphur, nitrogen, and hydrogen atoms are denoted as green, red, yellow, red, and grey balls. (Permission from ref. 66, Copyright 2018, Elsevier.)

thus-produced carbon materials with excellent conductivity and flexibility. At elevated temperatures, asphalt will become highly fluid, allowing the final structures of the carbon to be elaborately modulated through the interaction with deliberately introduced templates and/or other additives.<sup>57,60,61</sup> Moreover, the heteroatoms in resins and asphaltenes can lead to the production of heteroatom-doped carbon materials capable of pseudocapacitive energy harvest, a highly demanded property for rate-capable energy storage devices.<sup>64</sup> Because of the aforementioned advantages, asphalt holds great promise in constructing carbon materials for energy storage applications.

The representative heavy by-product from the conversion processes is petroleum coke,<sup>40,65</sup> which is usually formed during the cracking of hydrocarbon molecules around 400–500 °C.<sup>66</sup> With the heavy oil as the feedstock, the yield of petroleum coke can approach 10%, and even exceed 20% if extra-heavy oil is employed.<sup>39</sup> A large amount of petroleum coke is treated as fuel, especially in developing countries.<sup>39</sup> The combustion of such a heavy by-product can result in serious greenhouse gas emissions. Besides, petroleum coke usually contains high levels of sulphur and metal residuals that would cause very formidable environmental pollution in combustion processes.<sup>67</sup> As a result, alternative strategies are urgently needed to consume such a large amount of petroleum coke in an environment-friendly and value-added manner.<sup>68</sup> Normally, petroleum coke gives a carbon content as high as 80 wt%, and is made of stacked, linear, and curved PAH molecules decorated with heteroatoms and defects, as illustrated in Fig. 2.<sup>66</sup> In this regard, one viable solution may be the fusion of PAHs and isolation of them into graphene nanosheets.<sup>69</sup> Another possibility is to cut petroleum coke at defective sites into carbon quantum dots.<sup>70</sup> Previous results have demonstrated that both of these two nanostructured carbon materials are promising candidates for energy storage applications.<sup>71,72</sup> As a result, the establishment of reliable and cost-effective strategies to convert petroleum coke into graphene nanosheets and carbon quantum dots can be of paramount importance in its sustainable utilization.

### 3. Preparation methods of heavy oil-derived carbon materials

In general, the precursors are thermally annealed in an inert atmosphere to progressively liberate volatile matter and reorganize the remaining atoms, giving rise to carbon materials.<sup>22</sup> To exert elaborate control on the resulting carbon materials made from heavy oil-derived by-products for reliable energy storage applications, a multitude of manipulation strategies have been proposed in the past few years.

#### 3.1 Direct carbonization

Herein, direct carbonization refers to thermal annealing of the feedstock in an inert atmosphere without any additives.<sup>73</sup> The straightforwardness and simplicity make direct carbonization competitive in terms of cost and mass production.<sup>51</sup> To precisely control the structures of products from direct carbonization, pre-treatments, as well as the thermal annealing processes, should be delicately conducted based on the properties of the precursors.

One representative example of pre-treatment is the manipulation of asphalt into a mesophase as the precursor for mesocarbon microbeads (MCMBs).<sup>74</sup> MCMBs are micrometer-sized carbon spheres made of stacked graphene nanoplates. These structural merits provide MCMBs with a promising potential in a wealth of current and emerging applications including high-strength and high-density materials, column fillers, catalyst supports, and so on.<sup>75,76</sup> Their potential for direct lithium storage has been widely demonstrated.<sup>77</sup> Alternatively, they can also serve as excellent supports to load active species with poor conductivity, for example amorphous silica, for further enhanced lithium storage capability.<sup>78</sup> Generally, asphalt will

undergo uncontrolled melt and fusion at elevated temperatures that results in carbonized products with irregular structures and unsatisfactory properties.<sup>51</sup> To prepare MCMBs, asphalt must be pre-treated to manipulate the content of different fractions.<sup>79</sup> Typical pre-treatments include thermal polycondensation, catalytic polymerization, *etc.*<sup>79</sup> During these processes, the mesophase asphalt is formed which will then be gradually grown into spheres with suitable sizes before leaching out, giving rise to mesophase microbeads (MPMBs). The subsequent thermal annealing process also plays a critical role in determining the properties and practical performance of MCMBs. As a result, a delicate annealing procedure is generally proposed based on a thorough thermogravimetric analysis of MPMCs. Typically, a fast ramping rate is applied at relatively low temperatures, for example below 350 °C, as the microbeads remain quite stable in this temperature range. At elevated temperatures, the heating rate should be essentially reduced because of the liberation of small molecules. After that, a higher ramping rate could be restored as a stable structure is already formed. Another important parameter is the annealing temperature. The interlayer spacing of MCMBs is firstly increased and then decreased with continuously increasing the annealing temperature.<sup>80</sup> The reasons for the fluctuation are as follows. At relatively low temperatures, the release of small molecules will cause the turbulence of the stacked layers, which will inevitably expand the interlayer spacing. This trend normally extends to the heating temperature of around 900 °C. At higher temperatures, the preferred orientation of the graphene sheets will lead to the ordering of the stacked layers, giving rise to the decreased interlayer spacing.

Because of the relatively low yield of MPMBs, simplified pre-treatments are urgently required for cost-effective and mass-production of carbon materials with desired properties. Hu and his colleagues reported the fabrication of disordered carbon materials capable of sodium storage by carbonizing pre-oxidized asphalt. As shown in Fig. 3, the asphalt will melt and reorder at elevated temperatures, resulting in a well-organized stacking structure almost without porosity. To prevent heavy restacking, pre-oxidation has been proposed to introduce bridge bonds among these asphalt molecules which will limit their reordering at elevated temperatures, allowing the porosity to be inherited by the final carbon materials.<sup>51</sup> Another efficient strategy for producing this kind of disordered carbon material is to carbonize solvent extracted asphalt where fractions with low molecular weight are removed. Very recently, Hu's group reported an even more simplified means to produce disordered carbon materials by directly annealing asphalt at a precisely controlled temperature.<sup>73</sup>

Petroleum coke is generally formed at relatively low temperatures, which contains volatile matter ranging from 6 to 20 wt%. As a result, it must be processed at higher temperatures for a thermal upgrade before practical use. For the sake of producing carbon materials for energy storage applications, direct carbonization of petroleum coke is also one of the most straightforward strategies. There are quite some different types of petroleum cokes as they can be formed during different processes in the refinery. The rational selection of the suitable

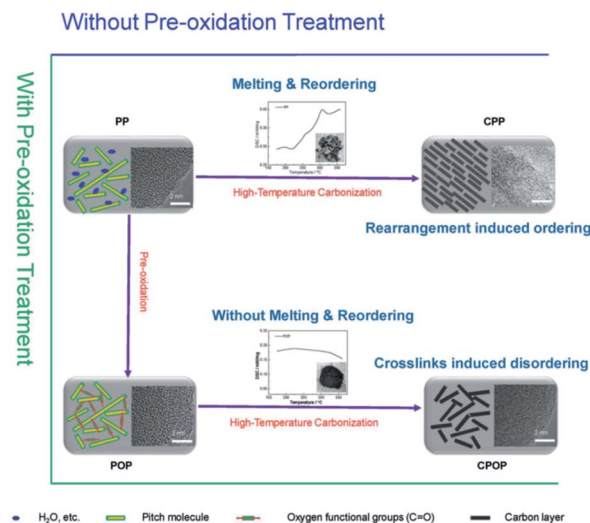


Fig. 3 Schematic comparison of carbon materials from asphalt precursors with and without pre-oxidation. (Permission from ref. 51, Copyright 2018, Wiley-VCH.)

one represents the first step. The annealing temperature also plays an important role in determining the structure of the final carbon materials. As a result, the origin of petroleum coke as well as the carbonization temperature should be carefully considered in the process of controlled production of carbon materials for real applications.

### 3.2 Activation

Carbon materials with large specific surface areas and high porosity are desperately needed for quite some energy storage applications. To this end, activation represents the most efficient and straightforward means and has been widely used. The activation process is usually carried out by calcining precursors in the presence of activation agents, for example KOH, in an inert atmosphere. During the heat treatment, multiple K-containing species such as  $K_2CO_3$  and  $K_2O$  will be generated and etch the matrix *via* redox reactions, leaving the carbonaceous framework with rich micro- and meso-pores behind. Besides, metallic K will also be produced through these reactions, which can intercalate into the carbon lattice, inducing distortion and expansion of carbon layers. Through the aforementioned processes, the specific surface area and porosity of the matrix can be significantly increased. J. Tour *et al.* reported the production of a high surface area activated porous carbon through carbonizing asphalt in the presence of KOH at 700 °C.<sup>49</sup> The as-obtained porous carbon offers a specific surface area of  $2780 \text{ m}^2 \text{ g}^{-1}$  and a pore volume as high as  $1.17 \text{ cm}^3 \text{ g}^{-1}$ . Besides KOH,  $ZnCl_2$ ,  $H_3PO_4$ , and  $H_2O$  have also been widely employed as activation agents in preparing porous carbon materials. Wu and his colleagues compared the effects of different activation agents.<sup>81</sup> In their research of activating petroleum coke, they found that the combined use of KOH and  $H_2O$  is more powerful in generating high specific surface areas than the sole employment of either KOH or  $H_2O$ . Another interesting finding in their research was that the metal impurity in petroleum coke

benefits the formation of large specific surface areas. Compared to petroleum coke with less metal impurity, the one with higher metal content led to the formation of porous carbons with a larger surface area.

Increasing the surface area will inevitably deteriorate the electrical conductivity of carbon materials. As a result, the traditional activation methods should be properly modified to exclude this adverse effect. In this regard, Kang *et al.* proposed the introduction of  $\text{FeCl}_3$  during the KOH-mediated activation of MCMBs where the Fe species could promote the localized graphitization during the etching process.<sup>82</sup> The as-formed graphitic region serves as an alternative electron transfer pathway, offsetting the etching-induced conductivity deterioration. The as-obtained carbon materials show a highly porous core covered by a graphitic shell (Fig. 4). As shown in Raman spectra (Fig. 4d), the exterior surface of particles gives a much stronger G band compared to the interior core which will favour fast charge transfer.

Despite their wide applicability, these activation processes are too harsh which will significantly reduce the density of the as-obtained porous carbon materials.<sup>83</sup> Moreover, the activation simultaneously proceeds *via* all directions and the as-formed pores are thus highly tortuous. As a result, controlled etching strategies are urgently required. Recently, catalytic hydrogenation of carbon has received renewed interest as a viable solution to create pores and tunnels in carbon materials.<sup>84</sup> At elevated temperatures, the hydrogen flow will etch carbon facilitated by the pre-anchored transition metal nanoparticles. In contrast to the traditional activation processes, the hydrogenation-induced etching proceeds along specific directions and the etching direction can be modulated by magnetic fields and the interaction with supporting substrates. Besides, quite some different transition metals, such as Ni, Fe, Co, Pt, and Ag, can be used as catalysts to promote hydrogenation.<sup>84</sup> Moreover, the size of the etched pore/tunnel is affected by the size of the catalyst particles. Through the combined use of these different effects, the introduced pores can be precisely controlled through this technology, enabling the activation of carbon materials in a desired manner. J. Cho *et al.* used Ni nanoparticles to etch MCMBs through the hydrogenation reaction and the as-formed particles are decorated with highly oriented pores without distortion.<sup>78</sup>

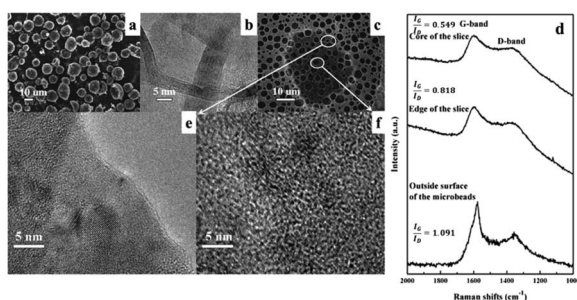


Fig. 4 Structural characterization of the activated MCMBs in the presence of  $\text{FeCl}_3$ : (a and c) SEM images, (b, e, and f) TEM images and (d) Raman Spectra. (Permission from ref. 77, Copyright 2013, Springer Nature.)

### 3.3 Co-carbonization

The structure of carbon materials is largely determined by the employed precursors. Thus, the rational selection of precursors represents an important means in the controlled construction of carbon materials with desired properties. Nevertheless, carbon materials from a single precursor, sometimes, cannot fully fulfil the practical requirements of many applications. As a result, the combined use of different precursors with distinct properties for the production of carbon materials has risen as a viable solution to address the bottleneck of single-precursor strategies.<sup>35,85</sup> In this context, the different structural merits can be collectively fused at micro-, nano-, and even atomic scales, thereby significantly extending the practical applications of carbon materials.

Co-carbonization has been used to produce soft-hard composite carbon.<sup>86–88</sup> Heavy by-products from the petroleum refinery are rich in PAHs, which are prone to form soft carbon consisting of stacked graphene layers with a high degree of ordering. These structural merits make soft carbon rate-capable anodes for lithium/sodium storage.<sup>89</sup> In contrast, polymers and biomass tend to be converted into hard carbon, which is bulky particles consisting of small-size graphene with poor ordering. Such a structural feature may provide more active sites for lithium and sodium storage, thus contributing to higher specific capacities. In fact, hard carbon represents the state-of-the-art carbon-based anode material for sodium-ion batteries.<sup>22</sup> Carbon materials synergistically combining the advantages of soft and hard carbons are a preferable choice for electrode materials for many energy storage applications. Their synthesis can be realized *via* the co-carbonization of asphalt and polymers/biomass. Li *et al.* reported the cost-effective fabrication of soft-hard composite carbon materials through a co-carbonization of asphalt and phenolic resin.<sup>90</sup> With a properly modulated formulation of the precursors, a hybridized carbon material with the uniformly mixed graphitic local region and turbostratic structure is formed. Then, the same group reported the fabrication of such a carbon material at a lower cost by replacing the phenolic resin with lignin.<sup>35</sup> The evolution of the local structure at different asphalt/lignin ratios and temperatures is exhibited in Fig. 5. As is shown, both higher annealing temperature and a larger portion of asphalt in the precursors result in extended graphitic regions, indicative of the high controllability of this method.

In addition to the formation of the soft-hard composite carbon, the co-carbonization method has also been extended to synthesize two-dimensional nanosheets with alternately stacked soft carbon and graphitic carbon nitride ( $\text{g-C}_3\text{N}_4$ ). Taylor *et al.* reported such a structure through annealing urea and asphalt simultaneously. During this process, urea would be converted into two-dimensional  $\text{g-C}_3\text{N}_4$  nanosheets which further mediate *in situ* loading of soft carbon nanosheets derived from asphalt on them.<sup>91</sup>

Considering the high yield of carbon from asphalt, one promising possibility is to construct carbon monolithic structures through carbonizing the composite of asphalt and organic monoliths. These organic monoliths generally give very low

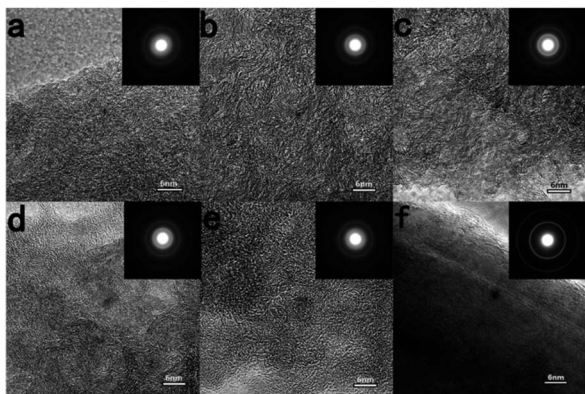


Fig. 5 Structural evolution of soft-hard composite carbon obtained by co-carbonization of asphalt and lignin with a mass ratio of 1 : 1 at (a) 1200, (b) 1400, and (c) 1600 °C as well as structures derived from precursors with mass ratios of (d) 7 : 3 and (e) 3 : 7. (f) TEM images of carbon derived from direct carbonization of asphalt at 1400 °C. (Permission from ref. 35, Copyright 2016, Royal Society of Chemistry.)

carbon yield and exclusive annealing of them at elevated temperatures would cause the collapse of the monolithic framework. With a suitable amount of asphalt introduced, the original macro-structure of the organic monolith can be well maintained. For example, Yang *et al.* reported such a monolithic structure through carbonizing asphalt coated melamine sponges and the final product offers excellent flexibility.<sup>92</sup> This structure affords a large surface area and high porosity for active species loading. Combined with its high conductivity and flexibility, it may hold great promise to serve as a current collector, capable of high mass loading, for electrodes of rechargeable batteries and supercapacitors, similar to graphene aerogels.<sup>93</sup>

### 3.4 Template method

Carbon materials with well-defined structures and morphologies are of particular importance for many energy-related applications.<sup>94</sup> As a result, precious control and manipulation of their shapes and other structural details have been highlighted as an important means to improve the practical performance of nanostructured carbon materials. Among all the available methods, the template-mediated synthesis has been regarded as the most straightforward technology.<sup>95,96</sup> In a typical process, the precursor, for example asphalt, is uniformly mixed with pre-synthesized templates or compounds that can be converted into templates with well-defined morphologies and then annealed at elevated temperatures, giving rise to carbon materials with expected structures after template removal.

The most widely employed templates include ZnO nanoparticles, MgO nanoplates,<sup>97</sup> SiO<sub>2</sub> nanospheres,<sup>98</sup> and so on.<sup>99</sup> One common feature of these templates is their high thermal stability which remains almost unchanged during the whole synthesis process. At the initial stage of annealing, the asphalt will become highly fluid and then uniformly and fully cover the templates at an optimal mass ratio of template and asphalt.<sup>57</sup> With further increase of temperature, the asphalt will be

gradually converted into carbon with an inverse replica of the template structure which finally contributes to nanostructured carbon materials with well-defined morphology, porosity, and so on. Wu *et al.* reported the synthesis of an ultrathin hollow carbon shell by employing commercial ZnO nanoparticles as the template.<sup>100</sup> At an optimal mass ratio of the precursor and template, the as-obtained carbon shell shows ultrathin thickness. Because of the wide availability of both the precursor and template, mass production of this carbon shell is possible. He's group proposed the synthesis of carbon nanosheets using MgO nanoplates as the template.<sup>101</sup> After removing the template, carbon nanosheets with a thickness of around 1 nm with highly wrinkled surfaces are obtained with a very high yield. The ultrathin thickness essentially shortens the diffusion path for ions/electrons, thus allowing the aforementioned carbon shells and nanosheets as rate-capable electrodes for supercapacitors, lithium-ion batteries, sodium-ion batteries, and so on.

SiO<sub>2</sub> nanospheres represent the most widely used template because of their facile synthesis procedure and high controllability. In this context, Wang and his colleagues prepared a honeycomb-like carbon material by using SiO<sub>2</sub> nanospheres as the template.<sup>102</sup> Due to the uniform size of the SiO<sub>2</sub> nanospheres, they can be closely packed into a superstructure and the melted asphalt would fill the void of the superstructure, giving rise to the honeycomb-like carbon material as shown in Fig. 6. Moreover, KOH has been simultaneously included to activate the carbon material for a large specific surface and hierarchical porosity. Such an architecture is highly desirable for capacitive energy harvest. Besides the possibility of manipulating the morphology of carbon materials, their composition can also be tuned by employing suitable templates. Wu *et al.* suggested the synthesis of an Fe-N-doped porous carbon framework using Fe<sub>2</sub>O<sub>3</sub> nanoparticles as the template. Some Fe species could be firmly confined with the carbon framework that survive the subsequent harsh acid etching for template removing.<sup>103</sup> These single metal-atom sites embedded in the carbon frameworks feature unsaturated coordination, and find applications in efficient electrocatalysis.<sup>104</sup>

The templates can also be introduced through the conversion reactions of some compounds, such as ferrocene,<sup>105</sup> melamine,<sup>106</sup> and citrate.<sup>64</sup> Although these compounds show ambiguous morphologies, they would be converted into templates with well-defined shapes directing the formation of carbon materials with anticipated structures. Song *et al.* annealed the mixture of asphalt and ferrocene in an autoclave

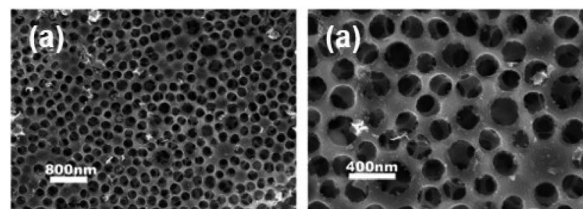


Fig. 6 (a) and (b) SEM images of honeycomb-like carbon synthesized using SiO<sub>2</sub> nanosphere templates. (Permission from ref. 102, Copyright 2018, Elsevier.)

during which the ferrocene was converted into Fe nanorods and the asphalt would be converted into hollow carbon nanotubes around the nanorods.<sup>105</sup> Melamine will condense into two-dimensional g-C<sub>3</sub>N<sub>4</sub> at elevated temperatures that can mediate the synthesis of two-dimensional carbon nanosheets. Moreover, the g-C<sub>3</sub>N<sub>4</sub> would be decomposed into active nitrogen-containing species at higher temperatures, facilitating the formation of nitrogen-doped carbon materials.<sup>107</sup> In our research, the uniformly mixed asphalt and melamine were annealed in a nitrogen atmosphere to give nitrogen-doped carbon nanosheets.<sup>106</sup> Other compounds can also be introduced simultaneously to construct dual and/or triple doped carbon nanosheets. For example, the direct annealing of asphalt, melamine, and phytic acid could give rise to nitrogen and phosphorus co-doped carbon nanosheets. Citrate would be decomposed into stacked carbonate particles that facilitate the formation of hierarchical carbon architectures.<sup>108</sup> In a typical example, the mixture of potassium citrate and asphalt with an optimal ratio was thermally treated.<sup>61</sup> The potassium citrate would be decomposed into potassium carbonate that serves as the *in situ* template, guiding the asphalt to form the nanosheet-assembled architecture. The potassium carbonate will be further decomposed into potassium oxide and carbon dioxide to activate the architecture, giving rise to a hierarchically porous structure. Even without employing the highly corrosive KOH as the activation agent, the as-obtained hierarchical carbon architecture can still give a specific surface area as large as 1200 m<sup>2</sup> g<sup>-1</sup> and porosity of 0.60 cm<sup>3</sup> g<sup>-1</sup>.

### 3.5 Molten salt method

Molten salt synthesis has recently been emerging as an intriguing technology to prepare nanostructured materials.<sup>83</sup> Molten salt refers to a salt that is in the solid state under ambient conditions but becomes liquid at elevated temperatures. A wide range of salt systems shows this property, thus providing versatile reaction environments. The molten salt synthesis combines the advantages of solution synthesis and solid-state reaction. On one hand, the liquid environment of molten salts can provide better heat control, sufficient dynamics, and facile reaction paths. On the other hand, the molten salts can create a high reaction temperature, which contributes to increased crystallinity for the as-synthesized materials. The unique reaction environment created by molten salt systems thus provides diverse control of the porosity, surface area, and morphology of carbon materials. Moreover, the introduction of extra additives can achieve the modulation of composition and graphitization of carbon materials. For example, the addition of nitrate into the LiCl/KCl molten salt system led to the formation of nitrogen-doped carbon while the introduction of sulphate results in the production of sulphur-doped carbon.<sup>109</sup> The content of heteroatoms within the carbon lattice can be tuned in a wide range. The promotion of graphitization was realized through intentionally adding iron containing salts through catalytic graphitization.<sup>110</sup> Another interesting feature of molten salt synthesis is the environmental friendliness since the salts can be easily

recycled from the final products *via* water washing for repeated use.<sup>111</sup>

For the first time, our group has employed this technology to produce heavy oil-derived carbon materials.<sup>60,111</sup> The heavy oil by-products, for example asphalt, were mixed uniformly with a eutectic salt made of NaCl and KCl, which can contribute to a liquid medium at temperatures higher than 657 °C. The melted salts create a flexible interface facilitating the dehydrogenation of PAHs which finally gives rise to large two-dimensional nanosheets. The direct carbonization of asphalt can only result in the formation of irregular carbon particles of several micrometers. Another interesting finding is the higher yield of carbon materials within the molten salt system. Specifically, the yield from direct carbonization of asphalt is 20.8 wt% while the molten salt system can offer a carbon yield of around 30 wt%. The reason may be due to the strong affinity of molten salt towards the organic species that leads to more precursors being converted. After the synthesis, the salts remain unchanged and can be recovered by simple water washing.<sup>111</sup> The recycled salts are available for repeated use. Another tunable molten salt synthesis has been realized *via* modulating the carbonization temperature. In the KCl and CaCl<sub>2</sub> molten system, porous carbon particles, carbon nanoplates, and carbon nanosheets with different thicknesses have been produced at different temperatures. As shown in Fig. 7, the porous particles are obtained at 550 °C. With the increase of temperature to 675 °C, carbon nanoplates are harvested. When the temperature reaches 800 °C, flexible carbon nanosheets are produced where the thickness of the nanosheets can be further reduced with increasing the temperature to 925 °C.<sup>60</sup> Because of the high controllability, the molten salt synthesis may serve as a promising strategy for the controlled synthesis of carbon materials cost-effectively. In addition, the continuous evolution of the structural merits makes the molten salt-mediated carbon materials an excellent platform to reveal the structure–performance relationships of electrode materials.

### 3.6 Defect-engineering synthesis

Defect-engineering synthesis suggested here refers to the technology that isolates nanomaterials from bulk materials by attacking their defective sites. This method has been widely employed to produce ultrafine nanomaterials, for example carbon quantum dots which are carbon particles smaller than

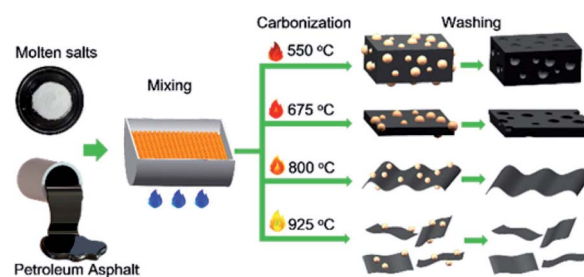


Fig. 7 Molten salt-mediated synthesis of nanostructured carbon with different morphologies. (Permission from ref. 60, Copyright 2018, American Chemical Society.)

10 nm with a crystalline inner core and functional groups on the outer surface.<sup>70,71,112</sup> The unique structure provides carbon dots with a wide range of applications including but not limited to photo- and electro-catalysis, lithium/sodium storage, and supercapacitors.<sup>71</sup> Petroleum coke is usually formed at relatively low temperatures. Despite the high carbon content and primary developed graphitic domain, the precursors still possess quite a lot of defects including heteroatoms, topological defects, *etc.*<sup>66</sup> These structural features allow the creation of carbon quantum dots using petroleum coke as the precursor. The chemical bonds at these defective sites are relatively weak, which will be tailored in advance under harsh conditions, thus permitting the ultrafine carbon particles to be isolated from the bulk petroleum coke and resulting in the formation of carbon quantum dots. We have successfully produced carbon quantum dots from petroleum coke *via* harsh oxidation using a mixed acid solution of H<sub>2</sub>SO<sub>4</sub> and HNO<sub>3</sub>.<sup>58</sup> The production was simply realized *via* refluxing the petroleum coke particles in these acids. These strong oxidative acids will first attack the defective sites which can simultaneously isolate ultrafine particles as well as anchor functional groups on their surfaces. Moreover, the functional groups can be simply regulated through changing the temperature. The carbon quantum dots synthesized at 120 °C mainly possess carbonyl and sulfonic groups while the products obtained at 180 °C are primarily decorated with sulfonic groups. The functional groups play a decisive role in determining the properties of the carbon quantum dots. As a result, the method suggested here may represent a simple, effective, and highly tunable means to produce carbon quantum dots. Besides, the carbon quantum dots can also be isolated from the bulk petroleum coke *via* a green electrolytic process.<sup>70</sup> In a typical synthesis, petroleum coke served as the working electrode and was electrolyzed in an ammonia electrolyte. Nitrogen-doped carbon quantum dots with uniform size distribution can be effectively and straightforwardly produced *via* this process as illustrated in Fig. 8. During the synthesis process, only ammonia-related ions are introduced, which can be facilely

removed, without any intractable ions in the synthesis system. As a result, the tedious dialysis process can be removed, allowing the essential simplification of the procedures for synthesizing carbon quantum dots.

## 4. Energy storage applications

Because of their excellent conductivity and diverse structures, carbon materials represent the most paramount electrode materials for electrochemical energy storage devices.<sup>32,36,113–115</sup> In these devices, carbon materials bridge the electron conduction and ion conduction which facilitates the conversion of chemical energy and electrical energy. However, these devices are operated using different mechanisms that impose distinct requirements on the structures and properties of carbon materials. For the sake of rational selection of suitable carbon-based electrode materials, an in-depth understanding of the relationship between the structure of carbon materials and their performance for certain applications is urgently required. In the following section, we will discuss the requirements on carbon materials in different applications based on the fundamental operation mechanisms of the dominating electrochemical energy storage devices including lithium-ion batteries, sodium-ion batteries, and supercapacitors as well as the capability of carbon materials from heavy oil derived by-products in fulfilling these requirements.

### 4.1 Lithium-ion batteries

Lithium-ion batteries are the dominant power sources for portable electronic devices as well as electric vehicles because of their light-weight and high energy density.<sup>116,117</sup> As a typical kind of rocking chair batteries, lithium ions are reversibly inserted and extracted between the two electrodes for energy storage and release, as shown in Fig. 9a.<sup>118</sup> Carbon materials, especially those with well-defined graphitic structures, have been widely employed as anodes for lithium-ion batteries where the inter-layer spacing provides favourable space for lithium ion accommodation.<sup>33</sup> Graphite anodes, as the most popular

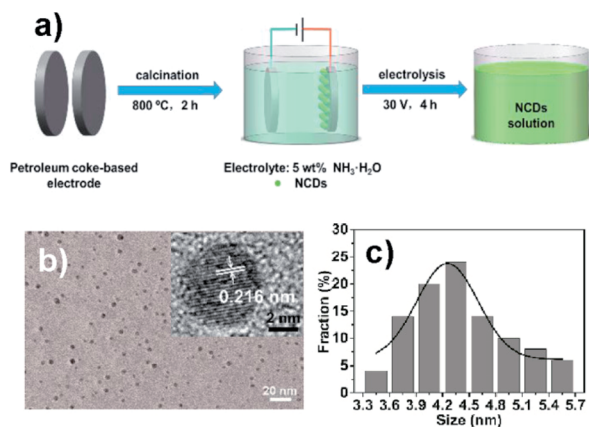


Fig. 8 (a) Schematic illustration of the synthesis of petroleum coke-based nitrogen-doped carbon dots (NCDs). (b) TEM and HRTEM images (inset) of NCDs. (c) The size distribution of NCDs obtained from multiple images. (Permission from ref. 70, Copyright 2018, Elsevier.)

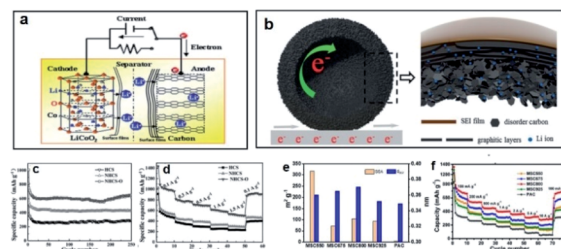


Fig. 9 (a) Schematic illustration of a lithium-ion battery. (Permission from ref. 118, Copyright 2011, Royal Society of Chemistry.) (b) Illustration of the asphalt-derived hybridized carbon shells for lithium storage and (c and d) the practical lithium storage performance based on this material. (Permission from ref. 129, Copyright 2016, Wiley-VCH.) (e) Comparison of specific surface area, interlayer spacing and (f) lithium storage performance of the samples obtained under different conditions. (Permission from ref. 60, Copyright 2018, American Chemical Society.)



anodes used today, are mainly made from petroleum coke, if not mined naturally. After calcination, the moisture and volatiles in the petroleum coke are largely removed. Then, thermal annealing at around 2800 °C for a long duration makes the artificial graphite ready for lithium storage.<sup>67,119</sup>

Despite the popularity of graphite as anodes for lithium storage, there are still quite some challenges needed to be addressed because of the increased requirements on better lithium-ion batteries by many emerging applications.<sup>33</sup> On the one hand, the outmost layers of graphite electrodes can be easily exfoliated *via* the repeated lithium insertion/deinsertion.<sup>120</sup> As a result, the appropriate modification should be conducted to improve the stability of graphite-based anodes. To this end, graphite anodes have been coated with asphalt-derived carbon, giving rise to carbon/graphite composites with improved properties.<sup>121</sup> After the formation of a less ordered graphitic layer on the graphite, not only the stability but also the initial coulombic efficiency has been enhanced, indicative of the potential of asphalt in boosting the performance of traditional electrodes. The improved initial Coulombic efficiency is mainly attributed to the blockage of the active edge sites of the pristine graphite *via* which the irreversible decomposition of electrolytes can be alleviated.<sup>122</sup> In a comparative study, asphalt with more heavy components has been demonstrated to be a preferable precursor to modulate graphite anodes for better practical performance.<sup>123</sup>

Another limitation of graphite anodes is their relatively small capacity. Theoretically, six carbon atoms can accommodate only one lithium ion which contributes to a theoretical capacity of 372 mA h g<sup>-1</sup>. For better fulfilling the increasing requirements of many current and emerging applications, anode materials with higher capacity are urgently demanded.<sup>33</sup> In this regard, MCMBs have been demonstrated as a favourable choice for anodes. Besides accommodation of lithium ions in the interlayer spacing, extra sites such as unstacked carbon layers and defects as well as the void between building blocks are also effective for lithium ion accommodation.<sup>124</sup> As a result, a reversible capacity as large as 500 mA h g<sup>-1</sup> is obtained, which is 50% higher than that of the graphite anodes.<sup>124</sup> Since then, tremendous research effort has been devoted to manipulating the performance of MCMB-based anodes for lithium storage. Ru *et al.* reported that the introduction of defects on the surface of MCMBs could effectively improve the lithium storage capacity.<sup>125</sup> Then, Jiang and his colleagues demonstrated that nitrogen doping of MCMBs is also capable of enhancing the specific capacity of the anodes.<sup>126</sup> The synergistic effect of the defective surface of MCMBs and nitrogen doping has been observed by Cui *et al.*<sup>127</sup> Specifically, the MCMBs were firstly oxidized using a modified Hummer's method to create defects. Then, the oxidized MCMBs were annealed in an ammonia atmosphere to dope with nitrogen. The thus-generated MCMBs deliver a specific capacity of almost 800 mA h g<sup>-1</sup>.

Hard carbon, which can be facily obtained from the heavy oil-derived by-product, has been evaluated for lithium storage.<sup>51</sup> Typically, hard carbons are generated using properly modulated asphalt, such as pre-oxidized and/or solvent extracted one.<sup>51</sup> These treatments allow the asphalt to be stable at elevated

temperatures without fusing into an extended conjugated region for the development of a large graphitic structure. Unlike the graphite anodes with only one insertion and extraction path for lithium ions, hard carbon normally shows a three-dimensional diffusion path for lithium ions enabling significantly improved rate capability.<sup>128</sup> Apart from the graphite anodes where the capacity is primarily harvested from the plateau between 0 and 0.2 V vs. Li/Li<sup>+</sup>, an obvious sloping region is generally observed from the charge–discharge curves of hard carbon-based anodes which leads to a decent amount of pseudocapacitive contribution for rate-capable lithium storage. For example, Wang *et al.* reported a high-power lithium-ion battery with hard carbon as the anode and a pseudocapacitive contribution as high as 94.5% is realized at a scan rate of 0.3 mV s<sup>-1</sup>.<sup>128</sup> The reason may be due to the synergistic effects of the three-dimensional lithium-ion diffusion path and multiple lithium accommodation sites.

In addition to these traditional anodes for lithium-ion batteries, quite some novel nanostructured carbon anodes have been prepared using heavy oil-derived by-products as the precursors for lithium storage. For example, Wu *et al.* prepared porous carbon frameworks using asphalt as the precursor and ZnO nanoparticles as the hard template.<sup>100</sup> The as-obtained products consist of ultrathin carbon nanosheet assembled architectures with interconnected pores enabling rapid ion transfer within the electrodes. Because of the rationally manipulated pore and morphology, the thus-produced carbon nanomaterials offer an excellent performance where a high capacity of around 400 mA h g<sup>-1</sup> is obtained at a current density of 1 A g<sup>-1</sup>. Then, Fe<sub>3</sub>O<sub>4</sub> nanoparticles have also been employed as the template to create such a porous network. Moreover, the existence of Fe species can promote the formation of graphitic regions at relatively low temperatures which can facilitate efficient electron conduction. Because of the aforementioned advantages, the anode based on this carbon material offers a high specific capacity of around 800 mA h g<sup>-1</sup> at a current density of 100 mA g<sup>-1</sup> and excellent cycling stability.<sup>44</sup> Wang *et al.* employed mesoporous SiO<sub>2</sub> sphere-mediated chemical vapour deposition to directly synthesize hybridized asphalt-derived carbon shells where the inner part is made of disordered carbon while the outer part consists of graphitic layers.<sup>129</sup> The thus-obtained carbon shells were modified with nitrogen through incorporating CH<sub>3</sub>CN as the nitrogen source. After activation with HNO<sub>3</sub> vapour, the electrode made of this material delivers a long-term stability and excellent rate performance, as shown in Fig. 9b–d. The rise of graphene has stimulated strong interest in storing lithium using two-dimensional carbon nanosheets. In this regard, Wei and his colleagues have carbonized asphaltene within a confined space, namely the interlayer spacing of vermiculite. The asphaltene molecules are then regularly joined together at the edges, thus giving rise to two-dimensional carbon nanosheets of several tens and even hundreds of micrometers.<sup>130</sup> Considering the wide availability and low cost of these precursors and the simple process, the two-dimensional carbon nanosheets synthesized through this technology are cheap enough to fulfil the requirement of electrode materials. Another interesting finding

## Review

in this research is the simple synthesis of CNT-graphene hybrid materials by introducing a certain amount of melamine together with asphaltene. During the heat treatment, melamine would be decomposed into reducing species at elevated temperatures which reduce the oxidative Fe species to iron particles. These particles can then catalyse the growth of CNTs seamlessly anchoring on the two-dimensional carbon nanosheets. These materials not only offer a high specific capacity of around  $800 \text{ mA h g}^{-1}$ , but also excellent rate capability where the capacity retention can be as high as 65% with a 20-fold increase of the current density.<sup>131</sup>

The practical performance of carbon materials for lithium storage is determined by quite some different factors, including crystallinity, particle size, porosity, morphology, hetero-species, and so on. To get a systematical understanding of their influences, the investigation of the lithium storage performance of distinct carbon materials from single sources as well as simple yet tunable strategies is required. Asphalt-derived carbon materials may be a promising platform for this purpose because of their excellent versatility in the construction of carbon materials as we mentioned before. Moreover, these totally different structured carbon materials can be obtained through a very simple process by changing only one parameter during the synthesis. For example, Wu and his colleagues produced a series of carbon materials from bulk particles and porous networks to ultrathin carbon nanosheets *via* a simple molten salt mediated synthesis.<sup>60</sup> The authors carefully compared the structural merits of different samples and their lithium storage properties in great detail. Fig. 9e and f show an interesting finding where a small specific surface area cannot secure high initial coulombic efficiency (ICE) as the sample with a specific surface area of  $4 \text{ m}^2 \text{ g}^{-1}$  offers a similar ICE to the one of around  $100 \text{ m}^2 \text{ g}^{-1}$ . Among all the parameters affecting the specific capacity, the interlayer spacing stands out. The specific capacity increases monotonously with the distance of interlayer spacing. Clearly, a higher interlayer spacing distance gives a larger specific capacity.<sup>60</sup> As a result, a suitable carbon anode for lithium storage should have a large interlayer spacing and a relatively large specific surface area.

Besides, asphalt has also been widely employed to hybridise with newly emerged anodes, such as silicon and metal oxides, to synergistically harvest the merits of different components for enhanced lithium storage. Wu *et al.* proposed a  $\text{ZnMn}_2\text{O}_4$  and porous carbon framework composite ( $\text{ZnMn}_2\text{O}_4/\text{PCF}$ ) by *in situ* growth of  $\text{ZnMn}_2\text{O}_4$  particles within the PCF from template-mediated carbonization of asphalt.<sup>132</sup> At the identical current density, the composite offers a larger specific capacity than that of PCF and  $\text{ZnMn}_2\text{O}_4$  particles. The synergetic effect may be ascribed to the improved dispersion of  $\text{ZnMn}_2\text{O}_4$  particles and the three-dimensional conductive network. In another attempt, Kang *et al.* coated  $\text{SnO}_2$ -CoO yolk-shell microspheres with asphalt-derived carbon offering significantly improved stability for lithium storage.<sup>133</sup> Very recently, Choi's group suggested that asphalt-derived carbon is more effective in alleviating the formidable volume variation of alloy anodes by systematically comparing the stability of carbon coatings from different precursors.<sup>57</sup> In addition to its economic advantages, asphalt

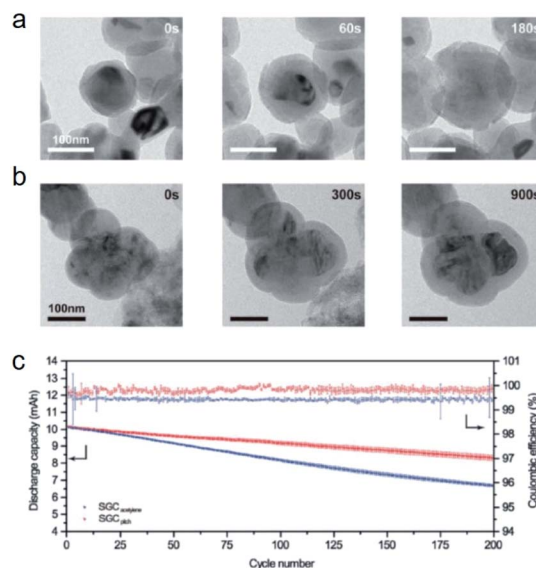


Fig. 10 *In situ* TEM internal pressurization lithiation measurement on (a) acetylene-derived carbon and (b) asphalt-derived carbon coated Si nanoparticles. (c) Comparison of the cycling stability of asphalt-derived carbon (red line) and acetylene-derived carbon coated Si-based anodes. (Permission from ref. 57, Copyright 2019, Wiley-VCH.)

offers a totally different carbonization behaviour that may facilitate the formation of a flexible structure for significantly improved stability. The carbon yield, which is highly associated with the mechanical strength, of asphalt is much higher than its polymer and biomass counterparts. Besides, the asphalt will become fluid allowing the molecules to be oriented for large stacked graphene nanosheets with high orientation. Such a structure is highly flexible and can survive the large volume variation of anode materials, for example silicon, without structural fracturation. As shown in the *in situ* TEM image of internal pressurization of lithiation in Fig. 10, the carbon coating layer derived from decomposed acetylene is easily cracked while the asphalt-derived carbon layer closely covering the silicon particles is expanded and shrunk synchronously with the silicon core without any breaks. Thus, the asphalt derived carbon-coated silicon particles show much improved cycling stability (Fig. 10c).

## 4.2 Sodium-ion batteries

Despite the multiple advantages of lithium-ion batteries, the scarcity and uneven distribution of lithium resources have severely hindered the wide deployment of lithium-ion batteries in large-scale energy storage facilitating the efficient utilization of intermittent renewable energy.<sup>22</sup> In this regard, sodium-ion batteries have attracted focused attention as a promising alternative to lithium-ion batteries technology.<sup>134,135</sup> Sodium-ion batteries show a configuration similar to that of lithium-ion batteries, as shown in Fig. 11a.<sup>136</sup> Sodium is an earth-abundant and evenly distributed element which can thus secure a reliable supply of the resource. Moreover, the higher redox potential of sodium enables the use of aluminum foil as

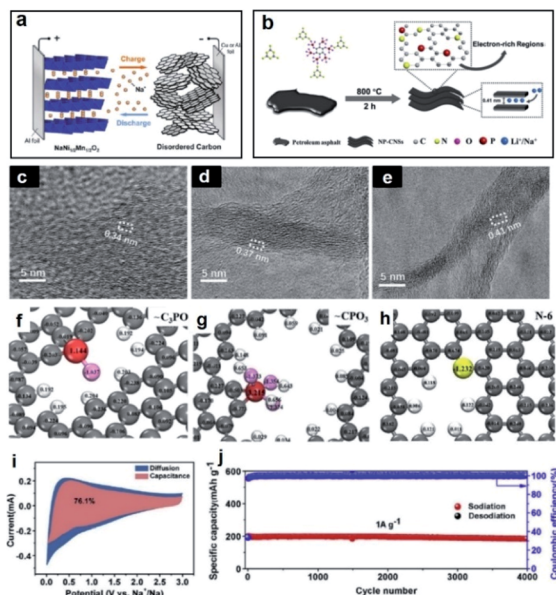


Fig. 11 (a) Typical configuration of a sodium-ion battery. (Permission from ref. 136, Copyright 2011, American Chemical Society.) (b) Schematic illustration of the carbon materials with tunable interlayer spacing. Interlayer spacing of petroleum-derived carbon (c), with nitrogen-doping (d), and nitrogen and phosphorus co-doping (e). Surface charge distribution modified by  $C_3PO$  (f),  $CPO_3$  (g), and N-6(h) functional groups. (i) Capacitive contribution of nitrogen and phosphorus co-doped carbon derived from asphalt at a scan rate of  $1.2 \text{ mV s}^{-1}$  and (j) the cyclic performance at a current density of  $1 \text{ A g}^{-1}$  for sodium storage. (Permission from ref. 106, Copyright 2019, Elsevier.)

the anode current collector, instead of copper foil required in lithium-ion batteries, which makes sodium-ion batteries more economically competitive. Finally, the adjacency of sodium to lithium in the periodic table makes the sodium-ion batteries the drop-in technology and the experiences in lithium-ion batteries development can be largely drawn. Nevertheless, there are still some differences between these two elements, which result in special issues for sodium-ion batteries needed to be addressed. For example, the higher redox potential of sodium makes the formation of sodium intercalated graphite thermodynamically unfavourable. As a result, the mature graphite anode for lithium-ion batteries technology is inapplicable for sodium-ion batteries and the exploration of suitable anodes represents the most significant challenge for sodium-ion batteries.

A very early anode for reversible sodium storage is soft carbon derived from petroleum coke, which was reported by Doeff *et al.*<sup>137</sup> However, the sodium storage sites of soft carbon are mainly located at the micropores and defects of the external surface, resulting in a relatively small specific capacity. To address this issue, hard carbon has been proposed for sodium storage as the internal micropores, expanded interlayer spacing, and defects are capable of sodium storage, enabling a much higher specific capacity.<sup>22</sup>

Then, quite some biomass and polymers have been employed as the precursors to produce hard carbon for sodium storage and decent performances have been widely reported. For example, Ji *et al.* reported a cellulose-derived hard carbon

with a reversible capacity of  $255 \text{ mA h g}^{-1}$  at a current density of  $40 \text{ mA g}^{-1}$ .<sup>138</sup> Nevertheless, the high price of these precursors has stimulated the search for more economical raw materials.<sup>35</sup> For the first time, Hu and his colleagues proposed that hard carbon can be facily synthesized by co-carbonizing the mixture of asphalt and lignin.<sup>35</sup> The lignin can emulsify asphalt which not only induces the formation of a disordered structure but also contributes to a high yield. The optimized product gives a reversible capacity of  $254 \text{ mA h g}^{-1}$  as well as excellent cycling stability. Other additives that facilitate the disordering of asphalt-derived carbon include phenolic resin, graphene oxide, *etc.*, and the thus-obtained materials exhibit excellent sodium storage performance. Since the first successful utilization of asphalt for preparing hard carbon to store sodium, Hu's group has elaborately designed a series of simple yet efficient technologies to produce asphalt-derived hard carbon with excellent performance. For example, defect-rich and disordered hard carbon can be facily prepared by bridging the asphalt molecules through oxygen bonds before carbonization.<sup>51</sup> As shown in Fig. 2, the as-prepared carbon gives a higher disorder that contributes to abundant internal micropores and defects. When evaluated as an anode for sodium storage, a high reversible capacity of around  $300 \text{ mA h g}^{-1}$  is delivered which almost remains unchanged after 200 cycles. The same group has also suggested that such an architecture could also be obtained by simply reducing the carbonizing temperature.<sup>73</sup> In particular, a carbonizing temperature higher than  $1000 \text{ }^\circ\text{C}$  generally leads to reordering of the asphalt molecules while at a lower temperature the driving force for this process is very weak. The product formed at  $800 \text{ }^\circ\text{C}$  gives excellent rate capability where a large capacity of around  $150 \text{ mA h g}^{-1}$  is still obtained even at a rate of  $12\text{C}$ .

Besides the microcrystal structure and defects, other structural parameters have also been rationally modulated for enhanced sodium storage. Xu and his colleagues reported a nano- $\text{CaCO}_3$  template method to create a three-dimensional framework made of asphalt derived carbon.<sup>89</sup> Moreover, the scaffold consists of the uniformly mixed disordered region and graphitic region. The high porosity can secure sufficient electrolyte penetration while the mixed scaffold allows simultaneously fast electron transfer and sufficient active sites for sodium storage. When evaluated as an anode for sodium storage, a reversible capacity of  $331 \text{ mA h g}^{-1}$  is obtained at a current density of  $30 \text{ mA g}^{-1}$ . With the almost 20-fold increase of the current density, the capacity retention is as high as 50%. Furthermore, a specific capacity of  $103 \text{ mA h g}^{-1}$  is retained after 3000 cycles at a current density of  $500 \text{ mA g}^{-1}$ . Yang and Yu's groups separately reported a more efficient template method.<sup>87,88</sup> In both cases, the phenolic resin has been introduced to modulate the distribution of the disordered region while the water-soluble salt, namely NaCl, has been used as the template to create the three-dimensional network made of carbon nano-sheets. The optimal structure gives a large reversible capacity of  $280 \text{ mA h g}^{-1}$  and a high initial coulombic efficiency of 75%. Moreover, such a structure can deliver excellent rate capability where the pseudocapacitive contribution is as high as 76% at a scan rate of  $1 \text{ mV s}^{-1}$  in the cyclic voltammetry evaluation.

The effects of surface charge and interlayer spacing on sodium storage have also been elaborately investigated. Our group has recently designed an *in situ* template and doping strategy to create carbon nanosheets with different surface charge distribution and interlayer spacing, which is illustrated in Fig. 11b.<sup>106</sup> Specifically, the two-dimensional morphology has been realized by carbonizing petroleum asphalt in the presence of melamine where the melamine could condense into two-dimensional graphitic-C<sub>3</sub>N<sub>4</sub> nanosheets as the template at elevated temperatures and the template can be decomposed at higher temperatures. Moreover, the surface charge and interlayer distance can be simply manipulated by incorporating different doping atoms such as nitrogen and phosphorus. For example, the directly carbonized asphalt shows an interlayer distance of 0.34 nm, while this value increases to 0.37 and 0.41 nm with nitrogen doping and nitrogen/phosphorus co-doping, respectively, as shown in Fig. 11c–e. Furthermore, the co-doping can create a negatively charged surface (Fig. 11f–h) which can facilitate sodium ion adsorption. In this regard, the co-doped carbon nanosheets show a capacity of 285 mA h g<sup>-1</sup> at a current density of 200 mA g<sup>-1</sup> and a pseudocapacitive contribution of 76.1% at a scan rate of 1.2 mV s<sup>-1</sup> (Fig. 11i). Even when cycled at a current density of 1 A g<sup>-1</sup> for 4000 times, a capacity retention of 94% is achieved (Fig. 11j), indicative of the excellent cycling stability. A similar contribution has also been observed by storing sodium using nitrogen/sulphur co-doped carbon materials.<sup>139,140</sup> Considering the possibility of facilely fabricating such materials by selecting the heavy by-products with inherent sulphur and nitrogen, nitrogen/sulphur co-doped carbon materials from heavy oils represent a promising choice for anodes for rate-capable sodium storage deserving exploration.

### 4.3 Supercapacitors

Batteries are capable of large energy output but with a poor power density. In modern society, energy storage devices with excellent power capability are indispensable for many applications such as electric tramcars, braking energy harvest, and gantry cranes.<sup>20,141</sup> Supercapacitors are a preferable choice of devices for this purpose because of their capability of fully delivering the stored charge within seconds. Unlike batteries where the charge is stored in the bulk phase of the electrode materials, supercapacitors only use the surface of electrode materials for charge storage either *via* electrostatic adsorption of ions or fast surface redox reactions, as shown in Fig. 12a.<sup>142</sup> In order to store as much charge as possible, electrode materials with a large specific surface area are the priority. To secure fast charge/discharge, electrode materials should possess high conductivity and low tortuous pores. As a result, porous carbons, especially those with hierarchical porosity, have been widely employed as electrodes for supercapacitors. Generally, macropores provide sufficient space as the electrolyte reservoir while mesopores and micropores are responsible for fast electrolyte diffusion and ion accommodation, respectively.<sup>143</sup> In the past decades, tremendous research effort has been devoted to this area with remarkable progress. Because of the high

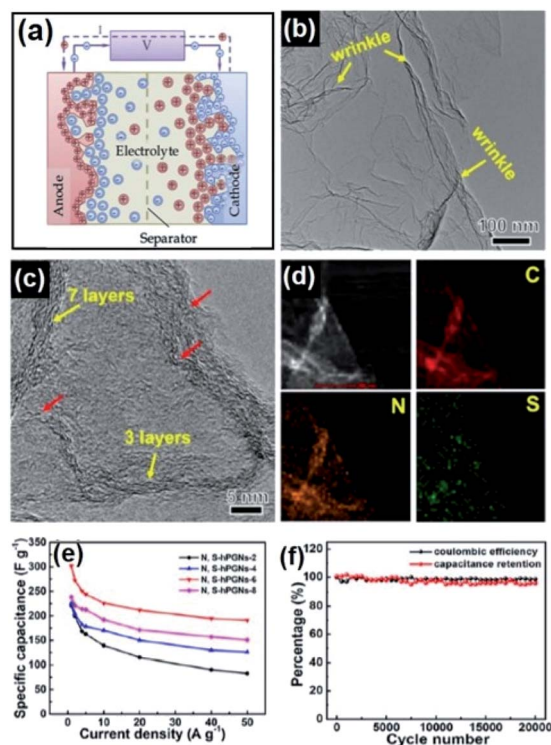


Fig. 12 (a) Scheme of a typical supercapacitor. (Permission from ref. 142, Copyright 2014, Elsevier.) (b and c) TEM images of nitrogen and sulphur co-doped carbon nanosheets and their elemental distribution (d). (e) Rate performance of nitrogen and sulphur co-doped carbon nanosheets with different heteroatom contents. (f) Long-term stability of optimized nitrogen and sulphur co-doped carbon nanosheets. (Permission from ref. 42, Copyright 2019, American Chemical Society).

tunability of heavy oil by-products in creating carbon materials, these carbon materials have been widely used for capacitive energy harvesting.<sup>2,68,144</sup>

To contribute to such a carbon architecture, KOH-mediated activation is the most straightforward technology. The carbon precursor, for example petroleum coke, is mixed with a large amount of KOH and annealed at elevated temperatures to create a large specific surface area and high porosity for electrostatic ion adsorption. Yang *et al.* reported a three-dimensional graphitized carbon nanovesicle architecture by simple activation of petroleum coke with KOH.<sup>145</sup> An unusual discovery is that such a structure mainly consists of highly graphitic pore walls made of three to four layers of graphene. The pores are mainly mesoporous which are suitable for large electrolyte ions. As such, an ionic liquid-based supercapacitor is assembled using this carbon material as the electrode with superior performance. The traditional KOH-activated carbon materials solely utilize ion adsorption for energy storage and surface redox reactions should also be rationally incorporated for further improved performance. In this regard, quite some post-treatments have been conducted on KOH-activated carbons for enhanced capacitive performance. Of particular note is the incorporation of heteroatoms, for example nitrogen, for essentially modulating the local electronic configuration and

chemical properties *via* which improved wettability, enhanced conductivity, and pseudocapacitive contribution could be expected.<sup>146</sup> In this regard, fundamentally boosted electrochemical performance is highly possible. For example, Wu and his colleagues reported the combination of KOH activation of petroleum coke with a subsequent ammonia hydrothermal modification. The as-obtained carbon materials contain a large number of nitrogen-containing species which can simultaneously improve the wettability and conductivity.<sup>147</sup> When evaluated as electrode materials for supercapacitors, an obviously pseudocapacitive contribution, as well as significantly improved rate capability, is observed. Besides these functional active species, redox couples have also been grafted on the surface of the KOH-activated carbons for a higher capability of surface charge storage. Yan *et al.* modified petroleum coke-derived carbon with hydroquinone/benzoquinone, the two-electron redox couple which almost leads to a two-fold increase of specific capacitance.<sup>144</sup> Specifically, an unprecedented specific value of  $300 \text{ F g}^{-1}$  is obtained for the redox couple modified carbon while the one without any modification only gives a specific capacitance of around  $160 \text{ F g}^{-1}$ .

Nevertheless, direct activation with KOH shows poor controllability in determining pore structures. As a result, the template-mediated synthesis has been coupled with KOH-activation which simultaneously increases the specific surface areas and modulates the pore structure. Wang and his colleagues reported a hierarchically porous carbon architecture from asphalt enabled by template mediated synthesis and simultaneous KOH activation.<sup>102</sup> The macropores inherited from hard templates can hold sufficient electrolytes that can be immediately transferred to microporous active sites *via* the adjacent mesopores, thus enabling outstanding capacitive performance. High specific capacitances of around 341 and  $189 \text{ F g}^{-1}$  are obtained at 1 and  $50 \text{ A g}^{-1}$ , respectively. Similar results have also been reported by our group in constructing such an architecture using KOH-activation of asphalt in a molten salt environment. Specifically, the petroleum asphalt was carbonized in the presence of KCl and KOH where the combined effect of molten salt, namely KCl and activation contributed to the carbon architectures with the desired morphology.<sup>148</sup> When evaluated as electrodes for supercapacitors, the as-obtained materials deliver an outstanding performance.

The rate capability of capacitive electrode materials can also be manipulated through constructing highly porous and ultrathin carbon nanosheets as the ultrathin thickness can significantly reduce the ion diffusion path for an enhanced rate performance. He's group employed two-dimensional MgO nanoplates for the direct synthesis of ultrathin carbon nanosheets and then creation of nanopores on these sheets through subsequent KOH-activation.<sup>101</sup> The optimal structure gives a specific capacitance of  $280 \text{ F g}^{-1}$  at a current density of  $0.05 \text{ A g}^{-1}$  and  $233 \text{ F g}^{-1}$  at  $20 \text{ A g}^{-1}$ . Similar conclusions have also been confirmed by Ning and Li's groups, separately.<sup>37,42</sup> Based on the aforementioned progress, the rational assembly of hierarchical architectures using two-dimensional carbon nanosheets as the sub-units represents a promising strategy to boost the electrode material performance in supercapacitors.

Recently, our group proposed an effective *in situ* technology to construct such an architecture as an electrode material for supercapacitors.<sup>61</sup> This architecture was simply obtained by annealing the mixture of asphalt and potassium citrate at an optimal mass ratio. The potassium citrate will first be decomposed into stacked potassium carbonate particles as the template and then be reduced to a wealth of activation agents such as  $\text{CO}_2$  and metallic potassium to create porosity. The facilely constructed three-dimensional carbon architecture made of porous carbon delivers robust capacitive energy storage performance in terms of a high specific capacitance ( $307 \text{ F g}^{-1}$  at  $0.05 \text{ A g}^{-1}$ ), an outstanding rate capability (73% capacitance retention at a 400-fold increase of current density), and favourable cycling stability (93.4% capacitance retention after 10 000 cycles). Li *et al.* introduced nitrogen and sulphur into hierarchical porous carbon nanosheets using graphitic carbon nitride as the template.<sup>42</sup> The high-sulphur asphalt served as the carbon source and sulphur source. As shown in Fig. 12b–f, the wrinkled carbon nanosheets are uniformly decorated with nitrogen and sulphur. When fabricated into a symmetrical supercapacitor, the thus-obtained device offers a large specific capacitance of  $302 \text{ F g}^{-1}$  at  $1 \text{ A g}^{-1}$  with 64% capacitance retention at a 50-fold increase of the current density. Moreover, the capacitance remains almost unchanged after 20 000 cycles.

## 5. Conclusions

Increasing amounts of heavy but low-cost by-products, such as asphalt and petroleum coke, are generated because more and more heavy oils are fed into the petroleum industry. This situation will remain unchanged in the foreseeable future despite the large deployment of new energy recently. As a result, how to realize harmonious development between the petroleum industry and new energy represents a vital challenge for researchers of different backgrounds. The employment of the heavy by-products as the precursors to construct novel carbon materials for energy storage applications may represent a viable means to bridge these two paradoxical fields. In this context, the undesirable heavy by-products can thus achieve value-added applications in the prospective new energy technology. After a brief introduction to the typical heavy oil-derived by-products, we summarized the recently proposed novel strategies for controlled construction of carbon materials with distinct structural merits. Through appropriate modulation, nanostructured carbon materials with different dimensions, diverse morphologies, tunable compositions, and so on have been successfully produced using these by-products as precursors. Then, their potential for electrochemical energy harvesting based on lithium-ion batteries, sodium-ion batteries, and supercapacitors has been elaborately analysed. In the past decades, remarkable progress has been achieved because of the tremendous effort devoted by researchers all over the world. Nevertheless, the rational utilization of heavy oil by-products to construct novel nanostructured carbon materials for robust energy storage still remains in its infancy and more improvements should be made to promote further development.

Heavy oil-based precursors should be carefully characterized for a better understanding of their conversion chemistry. Both asphalt and petroleum coke show complex components and structures and precursors of different origins may result in carbon materials with totally different structures *via* the same procedure. As a result, the in-depth understanding of precursors represents the fundamental for their controlled conversion into carbon materials with desired structures. To this end, the isolation of different group components is the primary step. The properties of these group components should be thoroughly characterized. Based on this basic knowledge, their joint characters should also be evaluated. Then, their carbonization behaviour should also be investigated in this manner, which can contribute to the establishment of the relationship between the features of the precursors and the structures of final products. The truly controlled construction of carbon materials in the desired manner could be possible based on this fundamental research.

As for the real application, industrial attention will be drawn only when competitive and reliable performance is obtained using commercial-level mass-loading ( $10 \text{ mg cm}^{-2}$ ) electrodes. Currently, most of the excellent electrochemical properties realized in lab research are recorded at a mass loading of  $1 \text{ mg cm}^{-2}$ , which is far from the requirement of the real application. The commercial-level mass loading usually results in electrodes as thick as  $200 \mu\text{m}$ . The diffusion length for the electrolyte would be quite long and the accessible surface area is reduced. The gravimetric performance of high mass loading is inevitably degraded especially at large charge/discharge rates. To address this issue, the as-obtained carbon materials should be elaborately assembled into integrated electrode architectures with fast electrolyte diffusion paths. Considering the distinct structural merits of carbon materials obtained *via* different strategies, targeted electrode architecture design rationales should be established based on the properties of the employed materials.

The rational design and controlled synthesis of carbon materials from heavy oil by-products for energy storage applications require a comprehensive understanding of heavy oil chemistry, chemical engineering, materials science and engineering, and electrochemistry. Joint research from researchers with different backgrounds including petrochemical engineering, analytical chemistry, materials science and engineering, and physical chemistry is needed. However, organizing such a team from industrial and scientific communities may be quite complex. As a result, the establishment of effective mechanisms to promote interdisciplinary cooperation is extremely important.

The feasibility of this field is also determined by environmental policies. With loose rules, decent profits could be made even by simply treating these by-products as fuels. Only under stringent requirements, the search for their clean and value-added utilization will be possible. Fortunately, serious environmental issues have caused worldwide attention which not only leads to strict policies but also attracts more and more research efforts devoted to this field.

The past decade has witnessed an increased interest in the search for cheap and tunable precursors to construct high-

performance carbon-based electrode materials for energy storage. Among them, heavy by-products from the petrochemical industry represent an appealing one because of their large amount and wide availability. Carbon materials derived from these precursors offer a wealth of advantages including high conductivity, tunable morphologies, *etc.* The related research may bridge the traditional petrochemical industry and the emerging new energy, where the rational combination of these two totally different fields may fundamentally address the real-world issues. Undoubtedly, promoting this research may be the “killing two birds with one stone” strategy that simultaneously addresses energy and environmental issues. With the gradually increased awareness on sustainable development of the whole society, it is highly believed that a clear roadmap of the value-added utilization of heavy oil by-products for producing energy storage materials is drawn and the breakthrough in this field will be witnessed in the near future.

## Conflicts of interest

There are no conflicts to declare.

## Acknowledgements

This work is financially supported by the National Natural Science Foundation of China (No. 21975287), the Thousand Young Talents Program of China, the Fundamental Research Funds for the Central Universities (19CX05002A), the Taishan Scholar Project (No. ts201712020), the Technological Leading Scholar of 10000 Talent Project (No. W03020508), the Shandong Provincial Natural Science Foundation (ZR2018ZC1458), and the start-up funding support of China University of Petroleum (East China).

## Notes and references

- 1 H. Chen, M. Ling, L. Hencz, H. Y. Ling, G. Li, Z. Lin, G. Liu and S. Zhang, *Chem. Rev.*, 2018, **118**, 8936–8982.
- 2 Y. Zhang, Y. Zhang, J. Huang, D. Du, W. Xing and Z. Yan, *Nanoscale Res. Lett.*, 2016, **11**, 245.
- 3 P. Simon and Y. Gogotsi, *Nat. Mater.*, 2008, **7**, 845–854.
- 4 S. Wang, G. Liu and L. Wang, *Chem. Rev.*, 2019, **119**, 5192–5247.
- 5 C. Yuan, H. B. Wu, Y. Xie and X. W. Lou, *Angew. Chem., Int. Ed.*, 2014, **53**, 1488–1504.
- 6 J. Yan, Q. Wang, T. Wei and Z. J. Fan, *Adv. Energy Mater.*, 2014, **4**, 1300816.
- 7 C. Liu, F. Li, L. P. Ma and H. M. Cheng, *Adv. Mater.*, 2010, **22**, E28–E62.
- 8 H. Wang, C. Zhu, D. Chao, Q. Yan and H. J. Fan, *Adv. Mater.*, 2017, **29**, 1702093.
- 9 J. Lang, X. Zhang, B. Liu, R. Wang, J. Chen and X. Yan, *J. Energy Chem.*, 2018, **27**, 43–56.
- 10 M. R. Lukatskaya, B. Dunn and Y. Gogotsi, *Nat. Commun.*, 2016, **7**, 12647.
- 11 B. C. Patra, S. Khilari, R. N. Manna, S. Mondal, D. Pradhan, A. Pradhan and A. Bhaumik, *ACS Catal.*, 2017, **7**, 6120–6127.

- 12 S. Bhunia, K. Bhunia, B. C. Patra, S. K. Das, D. Pradhan, A. Bhaumik, A. Pradhan and S. Bhattacharya, *ACS Appl. Mater. Interfaces*, 2019, **11**, 1520–1528.
- 13 S. Bhunia, S. K. Das, R. Jana, S. C. Peter, S. Bhattacharya, M. Addicoat, A. Bhaumik and A. Pradhan, *ACS Appl. Mater. Interfaces*, 2017, **9**, 23843–23851.
- 14 Y. L. Huang, Y. X. Zeng, M. H. Yu, P. Liu, Y. X. Tong, F. L. Cheng and X. H. Lu, *Small Methods*, 2018, **2**, 1700230.
- 15 H.-F. Wang and Q. Xu, *Matter*, 2019, **1**, 565–595.
- 16 W. H. Zuo, R. Z. Li, C. Zhou, Y. Y. Li, J. L. Xia and J. P. Liu, *Adv. Sci.*, 2017, **4**, 1600539.
- 17 X. Zhou, Q. Liu, C. Jiang, B. Ji, X. Ji, Y. Tang and H.-M. Cheng, *Angew. Chem., Int. Ed.*, 2019, **59**, 3802–3832.
- 18 G.-T. Xia, C. Li, K. Wang and L.-W. Li, *Sci. Adv. Mater.*, 2019, **11**, 1079–1086.
- 19 Y. Liu, G. Zhou, K. Liu and Y. Cui, *Acc. Chem. Res.*, 2017, **50**, 2895–2905.
- 20 Y. G. Wang, Y. F. Song and Y. Y. Xia, *Chem. Soc. Rev.*, 2016, **45**, 5925–5950.
- 21 H. Yuan, J.-Q. Huang, H.-J. Peng, M.-M. Titirici, R. Xiang, R. Chen, Q. Liu and Q. Zhang, *Adv. Energy Mater.*, 2018, **8**, 1802107.
- 22 D. Saurel, B. Orayech, B. Xiao, D. Carriazo, X. Li and T. Rojo, *Adv. Energy Mater.*, 2018, **8**, 1703268.
- 23 X.-B. Cheng, R. Zhang, C.-Z. Zhao and Q. Zhang, *Chem. Rev.*, 2017, **117**, 10403–10473.
- 24 H. Jiang, P. S. Lee and C. Li, *Energy Environ. Sci.*, 2013, **6**, 41–53.
- 25 Y. Lu, L. Yu and X. W. Lou, *Chem*, 2018, **4**, 972–996.
- 26 S. Zhang, Y. Zheng, X. Huang, J. Hong, B. Cao, J. Hao, Q. Fan, T. Zhou and Z. Guo, *Adv. Energy Mater.*, 2019, **9**, 1900081.
- 27 L. Feng, K. Wang, X. Zhang, X. Sun, C. Li, X. Ge and Y. Ma, *Adv. Funct. Mater.*, 2018, **28**, 1704463.
- 28 L. Yu, H. Hu, H. B. Wu and X. W. Lou, *Adv. Mater.*, 2017, **29**, 1604563.
- 29 C. Wang, L. Zhang, M. Al-Mamun, Y. Dou, P. Liu, D. Su, G. Wang, S. Zhang, D. Wang and H. Zhao, *Adv. Energy Mater.*, 2019, **9**, 1900909.
- 30 B. C. Patra, S. K. Das, A. Ghosh, A. Raj K, P. Moitra, M. Addicoat, S. Mitra, A. Bhaumik, S. Bhattacharya and A. Pradhan, *J. Mater. Chem. A*, 2018, **6**, 16655–16663.
- 31 L. L. Zhang and X. S. Zhao, *Chem. Soc. Rev.*, 2009, **38**, 2520–2531.
- 32 J. Wang, P. Nie, B. Ding, S. Dong, X. Hao, H. Dou and X. Zhang, *J. Mater. Chem. A*, 2017, **5**, 2411–2428.
- 33 L. Wang, J. Han, D. Kong, Y. Tao and Q.-H. Yang, *Nano-Micro Lett.*, 2019, **11**, 5.
- 34 Y. Zhang, X. Xia, B. Liu, S. Deng, D. Xie, Q. Liu, Y. Wang, J. Wu, X. Wang and J. Tu, *Adv. Energy Mater.*, 2019, **9**, 1803342.
- 35 Y. Li, Y.-S. Hu, H. Li, L. Chen and X. Huang, *J. Mater. Chem. A*, 2016, **4**, 96–104.
- 36 Z. Bi, Q. Kong, Y. Cao, G. Sun, F. Su, X. Wei, X. Li, A. Ahmad, L. Xie and C.-M. Chen, *J. Mater. Chem. A*, 2019, **7**, 16028–16045.
- 37 X. Song, X. Ma, Z. Yu, G. Ning, Y. Li and Y. Sun, *Chemelectrochem*, 2018, **5**, 1474–1483.
- 38 B. Dudley, *BP Energy Outlook*, BP p.l.c, 2019.
- 39 T. Wang, *Managing China's Petrocoke Problem*, 2015.
- 40 M. A. Fahim, T. A. Alsahhaf and A. Elkilani, in *Fundamentals of Petroleum Refining*, ed. M. A. Fahim, T. A. Alsahhaf and A. Elkilani, Elsevier, Amsterdam, 2010, pp. 1–9, DOI: 10.1016/B978-0-444-52785-1.00001-2.
- 41 A. Corma, E. Corresa, Y. Mathieu, L. Sauvanaud, S. Al-Bogami, M. S. Al-Ghrami and A. Bourane, *Catal. Sci. Technol.*, 2017, **7**, 12–46.
- 42 W. Yang, B. Deng, L. Hou, J. Tian, Y. Tang, S. Wang, F. Yang and Y. Li, *Ind. Eng. Chem. Res.*, 2019, **58**, 4487–4494.
- 43 M. Porto, P. Caputo, V. Loise, S. Eskandarsefat, B. Teltayev and C. Oliviero Rossi, *Appl. Sci.*, 2019, **9**, 742.
- 44 Y. Liu, P. Li, Y. Wang, J. Liu, Y. Wang, J. Zhang, M. Wu and J. Qiu, *J. Alloys Compd.*, 2017, **695**, 2612–2618.
- 45 W. A. Burgess and M. C. Thies, *Carbon*, 2011, **49**, 636–651.
- 46 A. Pradhan, P. Dechambenoit, H. Bock and F. Duroola, *Chem. – Eur. J.*, 2016, **22**, 18227–18235.
- 47 X.-Y. Wang, X. Yao and K. Müllen, *Sci. China: Chem.*, 2019, **62**, 1099–1144.
- 48 B.-J. Kim, Y. Eom, O. Kato, J. Miyawaki, B. C. Kim, I. Mochida and S.-H. Yoon, *Carbon*, 2014, **77**, 747–755.
- 49 A. S. Jalilov, G. D. Ruan, C. C. Hwang, D. E. Schipper, J. J. Tour, Y. L. Li, H. L. Fei, E. L. G. Samuel and J. M. Tour, *ACS Appl. Mater. Interfaces*, 2015, **7**, 1376–1382.
- 50 P.-Y. Zhao, J.-J. Tang and C.-Y. Wang, *J. Solid State Electrochem.*, 2017, **21**, 555–562.
- 51 Y. X. Lu, C. L. Zhao, X. G. Qi, Y. R. Qi, H. Li, X. J. Huang, L. Q. Chen and Y. S. Hu, *Adv. Energy Mater.*, 2018, **8**, 1800108.
- 52 P. Lu, Y. Sun, H. F. Xiang, X. Liang and Y. Yu, *Adv. Energy Mater.*, 2018, **8**.
- 53 T. Kawano, M. Kubota, M. S. Onyango, F. Watanabe and H. Matsuda, *Appl. Therm. Eng.*, 2008, **28**, 865–871.
- 54 F. Derbyshire, R. Andrews, D. Jacques, M. Jagtoyen, G. Kimber and T. Rantell, *Fuel*, 2001, **80**, 345–356.
- 55 A. H. Wazir and L. Kakakhel, *New Carbon Mater.*, 2009, **24**, 83–88.
- 56 J. Nai and X. W. Lou, *Adv. Mater.*, 2019, **31**, 1706825.
- 57 S. H. Choi, G. Nam, S. Chae, D. Kim, N. Kim, W. S. Kim, J. Ma, J. Sung, S. M. Han, M. Ko, H. W. Lee and J. Cho, *Adv. Energy Mater.*, 2019, **9**, 1803121.
- 58 X. Shao, W. Wu, R. Wang, J. Zhang, Z. Li, Y. Wang, J. Zheng, W. Xia and M. Wu, *J. Catal.*, 2016, **344**, 236–241.
- 59 Q. Zhao, H. Xie, H. Ning, J. Liu, H. Zhang, L. Wang, X. Wang, Y. Zhu, S. Li and M. Wu, *J. Alloys Compd.*, 2018, **737**, 330–336.
- 60 Y. Wang, W. Tian, L. Wang, H. Zhang, J. Liu, T. Peng, L. Pan, X. Wang and M. Wu, *ACS Appl. Mater. Interfaces*, 2018, **10**, 5577–5585.
- 61 L. Guan, L. Pan, T. Peng, T. Qian, Y. Huang, X. Li, C. Gao, Z. Li, H. Hu and M. Wu, *Carbon*, 2019, **152**, 537–544.
- 62 N. S. Mashaan, A. H. Ali, M. R. Karim and M. Abdelaziz, *Sci. World J.*, 2014, **2014**, 214612.
- 63 D. Lesueur, *Adv. Colloid Interface Sci.*, 2009, **145**, 42–82.

- 64 Z. Ling, Z. Wang, M. Zhang, C. Yu, G. Wang, Y. Dong, S. Liu, Y. Wang and J. Qiu, *Adv. Funct. Mater.*, 2016, **26**, 111–119.
- 65 J. Xiao, Q. Zhong, F. Li, J. Huang, Y. Zhang and B. Wang, *Energy Fuels*, 2015, **29**, 3345–3352.
- 66 Q. Zhong, Q. Mao, L. Zhang, J. Xiang, J. Xiao and J. P. Mathews, *Carbon*, 2018, **129**, 790–802.
- 67 A. A. Boateng, in *Rotary Kilns*, ed. A. A. Boateng, Butterworth-Heinemann, Boston, 2nd edn, 2016, pp. 265–290, DOI: 10.1016/B978-0-12-803780-5.00011-3.
- 68 J. F. Huang, W. Xing, F. Subhan, X. L. Gao, P. Bai, Z. Liu, Y. H. Wang, Q. Z. Xue and Z. F. Yan, *J. Mater. Res.*, 2017, **32**, 1248–1257.
- 69 M. Wu, Y. Liu, Y. Zhu, J. Lin, J. Liu, H. Hu, Y. Wang, Q. Zhao, R. Lv and J. Qiu, *J. Mater. Chem. A*, 2017, **5**, 11331–11339.
- 70 Y. Rao, H. Ning, X. Ma, Y. Liu, Y. Wang, H. Liu, J. Liu, Q. Zhao and M. Wu, *Carbon*, 2018, **129**, 335–341.
- 71 C. Hu, M. Li, J. Qiu and Y.-P. Sun, *Chem. Soc. Rev.*, 2019, **48**, 2315–2337.
- 72 Q. Zhou, Z. Zhao, Y. Zhang, B. Meng, A. Zhou and J. Qiu, *Energy Fuels*, 2012, **26**, 5186–5192.
- 73 Y. Qi, Y. Lu, F. Ding, Q. Zhang, H. Li, X. Huang, L. Chen and Y.-S. Hu, *Angew. Chem., Int. Ed.*, 2019, **58**, 4361–4365.
- 74 H. Xia, J. Hu, J. Li and K. Wang, *RSC Adv.*, 2019, **9**, 7004–7014.
- 75 D. Zhang, L. Zhang, X. Fang, Z. Xu, X. Sun and S. Zhao, *Fuel*, 2019, **237**, 753–762.
- 76 W. Yuan, Z. Qiu, Y. Huang, C. Wang, H. Huang, Y. Yang, X. Zhang, J. Luo and Y. Tang, *Energy Technol.*, 2019, **7**, 1900445.
- 77 Y. Lei, Z. H. Huang, Y. Yang, W. C. Shen, Y. P. Zheng, H. Y. Sun and F. Y. Kang, *Sci. Rep.*, 2013, **3**, 2477.
- 78 N. Kim, S. Chae, J. Ma, M. Ko and J. Cho, *Nat. Commun.*, 2017, **8**, 812.
- 79 I. Mochida, Y. Korai, C.-H. Ku, F. Watanabe and Y. Sakai, *Carbon*, 2000, **38**, 305–328.
- 80 T. Li, C. Wang, X. Liu, J. Zheng and H. Wang, *Chin. Sci. Bull.*, 2004, **49**, 1105–1110.
- 81 M. Wu, Q. Zha, J. Qiu, X. Han, Y. Guo, Z. Li, A. Yuan and X. Sun, *Fuel*, 2005, **84**, 1992–1997.
- 82 L. Ye, Q. H. Liang, Y. Lei, X. L. Yu, C. P. Han, W. C. Shen, Z. H. Huang, F. Y. Kang and Q. H. Yang, *J. Power Sources*, 2015, **282**, 174–178.
- 83 X. Liu, N. Fechner and M. Antonietti, *Chem. Soc. Rev.*, 2013, **42**, 8237–8265.
- 84 M. Lukas, V. Meded, A. Vijayaraghavan, L. Song, P. M. Ajayan, K. Fink, W. Wenzel and R. Krupke, *Nat. Commun.*, 2013, **4**, 1379.
- 85 Y. Cheng, Q. Zhang, C. Fang, Y. Ouyang, J. Chen, X. Yu and D. Liu, *J. Anal. Appl. Pyrolysis*, 2018, **129**, 154–161.
- 86 F. Xie, Z. Xu, A. C. S. Jensen, H. Au, Y. Lu, V. Araullo-Peters, A. J. Drew, Y.-S. Hu and M.-M. Titirici, *Adv. Funct. Mater.*, 2019, **29**, 1901072.
- 87 D. Qiu, T. Cao, J. Zhang, S.-W. Zhang, D. Zheng, H. Wu, W. Lv, F. Kang and Q.-H. Yang, *J. Energy Chem.*, 2019, **31**, 101–106.
- 88 P. Lu, Y. Sun, H. Xiang, X. Liang and Y. Yu, *Adv. Energy Mater.*, 2018, **8**, 1702434.
- 89 B. Cao, H. Liu, B. Xu, Y. Lei, X. Chen and H. Song, *J. Mater. Chem. A*, 2016, **4**, 6472–6478.
- 90 Y. Li, L. Mu, Y.-S. Hu, H. Li, L. Chen and X. Huang, *Energy Storage Mater.*, 2016, **2**, 139–145.
- 91 G.-M. Weng, Y. Xie, H. Wang, C. Karpovich, J. Lipton, J. Zhu, J. Kong, L. D. Pfefferle and A. D. Taylor, *Angew. Chem., Int. Ed.*, 2019, **58**, 13727–13733.
- 92 P. Zhao, Q. Yao, G. Zhou, X. Yan, S. Li, X. Dou and M. Yang, *Mater. Chem. Phys.*, 2019, **226**, 235–243.
- 93 J. Mao, J. Iocozzia, J. Huang, K. Meng, Y. Lai and Z. Lin, *Energy Environ. Sci.*, 2018, **11**, 772–799.
- 94 L. Wang, Y. Zhou and J. Qiu, *Microporous Mesoporous Mater.*, 2013, **174**, 67–73.
- 95 J. Lee, S. Han and T. Hyeon, *J. Mater. Chem.*, 2004, **14**, 478–486.
- 96 G. Ning, X. Ma, X. Zhu, Y. Cao, Y. Sun, C. Qi, Z. Fan, Y. Li, X. Zhang, X. Lan and J. Gao, *ACS Appl. Mater. Interfaces*, 2014, **6**, 15950–15958.
- 97 C. Tang, B. Wang, H.-F. Wang and Q. Zhang, *Adv. Mater.*, 2017, **29**, 1703185.
- 98 A. Vu, X. Li, J. Phillips, A. Han, W. H. Smyrl, P. Bühlmann and A. Stein, *Chem. Mater.*, 2013, **25**, 4137–4148.
- 99 X.-Y. Yu, H. Hu, Y. Wang, H. Chen and X. W. Lou, *Angew. Chem., Int. Ed.*, 2015, **54**, 7395–7398.
- 100 X. He, Z. Liu, H. Ma, N. Zhang, M. Yu and M. Wu, *Microporous Mesoporous Mater.*, 2016, **236**, 134–140.
- 101 X. He, N. Zhang, X. Shao, M. Wu, M. Yu and J. Qiu, *Chem. Eng. J.*, 2016, **297**, 121–127.
- 102 P. Abudu, L. Wang, M. Xu, D. Jia, X. Wang and L. Jia, *Chem. Phys. Lett.*, 2018, **702**, 1–7.
- 103 J. Liu, Y. Liu, P. Li, L. Wang, H. Zhang, H. Liu, J. Liu, Y. Wang, W. Tian, X. Wang, Z. Li and M. Wu, *Carbon*, 2018, **126**, 1–8.
- 104 Y. Pan, C. Zhang, Z. Liu, C. Chen and Y. Li, *Matter*, 2020, **2**, 78–110.
- 105 J. Zhou, H. Song, X. Chen, L. Zhi, S. Yang, J. Huo and W. Yang, *Chem. Mater.*, 2009, **21**, 2935–2940.
- 106 C. Gao, J. Feng, J. Dai, Y. Pan, Y. Zhu, W. Wang, Y. Dong, L. Cao, L. Guan, L. Pan, H. Hu and M. Wu, *Carbon*, 2019, **153**, 372–380.
- 107 Q. Lai, Q. Su, Q. Gao, Y. Liang, Y. Wang, Z. Yang, X. Zhang, J. He and H. Tong, *ACS Appl. Mater. Interfaces*, 2015, **7**, 18170–18178.
- 108 B. Yang, J. Chen, S. Lei, R. Guo, H. Li, S. Shi and X. Yan, *Adv. Energy Mater.*, 2018, **8**, 1702409.
- 109 X. Liu and M. Antonietti, *Adv. Mater.*, 2013, **25**, 6284–6290.
- 110 X. Liu, C. Giordano and M. Antonietti, *Small*, 2014, **10**, 193–200.
- 111 Y. Wang, Y. Wang, J. Liu, L. Pan, W. Tian, M. Wu and J. Qiu, *Carbon*, 2017, **122**, 344–351.
- 112 H. Wang, G. Ning, X. He, X. Ma, F. Yang, Z. Xu, S. Zhao, C. Xu and Y. Li, *Nanoscale*, 2018, **10**, 21492–21498.
- 113 M. Zeiger, N. Jäckel, V. N. Mochalin and V. Presser, *J. Mater. Chem. A*, 2016, **4**, 3172–3196.
- 114 K. L. Van Aken, C. R. Pérez, Y. Oh, M. Beidaghi, Y. Joo Jeong, M. F. Islam and Y. Gogotsi, *Nano Energy*, 2015, **15**, 662–669.



- 115 J. Niu, R. Shao, M. Liu, Y. Zan, M. Dou, J. Liu, Z. Zhang, Y. Huang and F. Wang, *Adv. Funct. Mater.*, 2019, **29**, 1905095.
- 116 H. Liu, G. Liang, C. Gao, S. Bi, Q. Chen, Y. Xie, S. Fan, L. Cao, W. K. Pang and Z. Guo, *Nano Energy*, 2019, **66**, 104100.
- 117 J. B. Goodenough and K.-S. Park, *J. Am. Chem. Soc.*, 2013, **135**, 1167–1176.
- 118 V. Etacheri, R. Marom, R. Elazari, G. Salitra and D. Aurbach, *Energy Environ. Sci.*, 2011, **4**, 3243–3262.
- 119 H. Marsh and F. Rodríguez-Reinoso, in *Activated Carbon*, ed. H. Marsh and F. Rodríguez-Reinoso, Elsevier Science Ltd, Oxford, 2006, pp. 454–508, DOI: 10.1016/B978-008044463-5/50023-6.
- 120 J. Ming, Z. Cao, W. Wahyudi, M. Li, P. Kumar, Y. Wu, J.-Y. Hwang, M. N. Hedhili, L. Cavallo, Y.-K. Sun and L.-J. Li, *ACS Energy Lett*, 2018, **3**, 335–340.
- 121 Y.-y. Zhou, X.-h. Li, H.-j. Guo, Z.-x. Wang, Y. Yang and Q.-l. Xie, *J. Cent. South Univ. Technol.*, 2007, **14**, 651–655.
- 122 Y.-J. Han, J. Kim, J.-S. Yeo, J. C. An, I.-P. Hong, K. Nakabayashi, J. Miyawaki, J.-D. Jung and S.-H. Yoon, *Carbon*, 2015, **94**, 432–438.
- 123 Y. J. Jo and J. D. Lee, *Korean J. Chem. Eng.*, 2019, **36**, 1724–1731.
- 124 I. Mochida, C.-H. Ku, S.-H. Yoon and Y. Korai, *J. Power Sources*, 1998, **75**, 214–222.
- 125 D. Zhao, Q. Ru, S. Hu and X. Hou, *Ionics*, 2017, **23**, 897–905.
- 126 Z. Zou and C. Jiang, *J. Mater. Sci. Technol.*, 2019, **35**, 644–650.
- 127 P. Han, Y. Yue, L. Zhang, H. Xu, Z. Liu, K. Zhang, C. Zhang, S. Dong, W. Ma and G. Cui, *Carbon*, 2012, **50**, 1355–1362.
- 128 H. C. Yu, X. L. Dong, Y. Pang, Y. G. Wang and Y. Y. Xia, *Electrochim. Acta*, 2017, **228**, 251–258.
- 129 Q. Ma, L. Wang, W. Xia, D. Jia and Z. Zhao, *Chem. – Eur. J.*, 2016, **22**, 2339–2344.
- 130 C. G. Xu, G. Q. Ning, X. Zhu, G. Wang, X. F. Liu, J. S. Gao, Q. Zhang, W. Z. Qian and F. Wei, *Carbon*, 2013, **62**, 213–221.
- 131 C. Xu, G. Ning, X. Zhu, G. Wang, X. Liu, J. Gao, Q. Zhang, W. Qian and F. Wei, *Carbon*, 2013, **62**, 213–221.
- 132 P. Li, J. Liu, Y. Liu, Y. Wang, Z. Li, W. Wu, Y. Wang, L. Yin, H. Xie, M. Wu, X. He and J. Qiu, *Electrochim. Acta*, 2015, **180**, 164–172.
- 133 J. H. Choi, G. D. Park, D. S. Jung and Y. C. Kang, *Chem. Eng. J.*, 2019, **369**, 726–735.
- 134 Y. Fang, X.-Y. Yu and X. W. Lou, *Matter*, 2019, **1**, 90–114.
- 135 C. Guo, W. Zhang, Y. Liu, J. He, S. Yang, M. Liu, Q. Wang and Z. Guo, *Adv. Funct. Mater.*, 2019, **29**, 1901925.
- 136 S. Komaba, T. Ishikawa, N. Yabuuchi, W. Murata, A. Ito and Y. Ohsawa, *ACS Appl. Mater. Interfaces*, 2011, **3**, 4165–4168.
- 137 M. M. Doeff, Y. Ma, S. J. Visco and L. C. De Jonghe, *J. Electrochem. Soc.*, 1993, **140**, L169–L170.
- 138 W. Luo, J. Scharadt, C. Bommier, B. Wang, J. Razink, J. Simonsen and X. Ji, *J. Mater. Chem. A*, 2013, **1**, 10662–10666.
- 139 J. Yang, X. Zhou, D. Wu, X. Zhao and Z. Zhou, *Adv. Mater.*, 2017, **29**, 1604108.
- 140 Y. Ma, Q. Guo, M. Yang, Y. Wang, T. Chen, Q. Chen, X. Zhu, Q. Xia, S. Li and H. Xia, *Energy Storage Mater*, 2018, **13**, 134–141.
- 141 J. R. Miller and P. Simon, *Science*, 2008, **321**, 651–652.
- 142 H. D. Yoo, E. Markevich, G. Salitra, D. Sharon and D. Aurbach, *Mater. Today*, 2014, **17**, 110–121.
- 143 D. W. Wang, F. Li, M. Liu, G. Q. Lu and H. M. Cheng, *Angew. Chem., Int. Ed.*, 2009, **48**, 1525.
- 144 Y. Zhang, T. Cai, J. Huang, W. Xing and Z. Yan, *J. Mater. Res.*, 2016, **31**, 3723–3730.
- 145 C. X. Peng, Z. B. Wen, Y. Qin, L. Schmidt-Mende, C. Z. Li, S. H. Yang, D. L. Shi and J. H. Yang, *ChemSusChem*, 2014, **7**, 777–784.
- 146 M. Yang and Z. Zhou, *Adv. Sci.*, 2017, **4**, 1600408.
- 147 M. Tan, P. Li, J. Zheng, T. Noritatsu and M. Wu, *New Carbon Mater.*, 2016, **31**, 343–351.
- 148 L. Pan, Y. Wang, H. Hu, X. Li, J. Liu, L. Guan, W. Tian, X. Wang, Y. Li and M. Wu, *Carbon*, 2018, **134**, 345–353.